

## METALLOPROTEINS WITH PHENOLATE COORDINATION

LAWRENCE QUE, JR.

*Department of Chemistry, Baker Laboratory, Cornell University, Ithaca, NY 14853 (U.S.A.)*

(Received 1 April 1982)

### CONTENTS

A. Introduction	74
B. Transferrins	74
C. Uteroferrin and purple phosphatases	81
D. Catechol dioxygenases	85
(i) Intradiol dioxygenases	86
(ii) Extradiol dioxygenases	98
E. Heme proteins with phenolate coordination	100
F. Summary	102
Acknowledgements	102
Note added in proof	102
References	104

### ABBREVIATIONS

EHPG	ethylenebis( <i>o</i> -hydroxyphenylglycine)
NBS	<i>N</i> -bromosuccinimide
Et <sub>2</sub> dtc	diethyldithiocarbamate
PCD	protocatechuate 3,4-dioxygenase
CTD	catechol 1,2-dioxygenase
catH <sub>2</sub>	catechol
OAc	acetate
salen	ethylenebis(salicylideneimine)
saloph	<i>o</i> -phenylenebis(salicylideneimine)
DBcatH <sub>2</sub>	3,5-di- <i>t</i> -butylcatechol
DBSQ	3,5-di- <i>t</i> -butyl- <i>o</i> -benzosemiquinone
HbM	mutant hemoglobin
His	histidine
Tyr	tyrosine
DSS	2,2-dimethyl-2-silapentane-5-sulfonate
DPXDM	deuteroporphyrin IX dimethyl ester
PPIXDBE	protoporphyrin IX di- <i>n</i> -butyl ester
SCE	saturated calomel electrode

## A. INTRODUCTION

The coordination chemistry of metal centers in metalloproteins has been an area of considerable interest for many years. Much of the chemistry has focused on thiolate and porphyrin complexes because of the ubiquity of metal-sulfur and heme containing proteins. In the past decade, however, a number of metalloproteins exhibiting phenolate coordination have been discovered; the presence of the phenolate in many cases imparts unique properties to the metal complex. This review will discuss several classes of proteins where phenolate coordination has been established unequivocally. These include non-heme iron proteins such as transferrin, uteroferrin, beef spleen purple phosphatase, and the catechol dioxygenases, the manganese containing purple phosphatases, and heme proteins such as the mutant hemoglobins and catalase. This review covers the literature to June, 1982.

## B. TRANSFERRINS

The transferrins are a class of transport proteins of molecular weight ca. 80,000 which display an extraordinary avidity for ferric ion [1-3]. The bound iron thus is protected from hydrolysis [4] and chelation by other biological components. These proteins have been purified from serum, egg-white and milk, among other fluids, and appropriately named serotransferrin,

TABLE I  
Resonance Raman data for metal-tyrosinate proteins

Protein	$\lambda_{\max}$ (nm)	Vibrational modes ( $\text{cm}^{-1}$ )				Ref.
Fe(III)-serotransferrin	465	1174	1288	1508	1613	23
Cu(II)-serotransferrin	435	1174	1281	1506	1608	23
Mn(III)-serotransferrin	430	1173	1264	1501	1603	24
Co(III)-serotransferrin	405	1164	1248	1493	1600	24
Fe(III)-ovotransferrin	465	1170	1270	1504	1605	24
Fe(III)-lactoferrin	465	1170	1272	1500	1604	25
Purple uteroferrin	550	1168	1285	1503	1603	78, 79
Pink uteroferrin	508	1169	1293	1504	1604	79
Sweet potato purple phosphatase	515		1298	1508	1620	89, 91
Protocatechuate 3,4-dioxygenase	460	1176	1265	1505	1605	80, 83, 84, 95
Catechol 1,2-dioxygenase	455	1175	1289	1506	1604	96, 97

ovotransferrin and lactoferrin, respectively. There are two metal binding sites with somewhat differing affinities for metal [5–7]; these appear sufficiently flexible to accommodate other metal ions [2,8–10] including Cu(II), Cr(III), Mn(III) and Co(III). Remarkably, the metal binding is accompanied by the binding of an equivalent of bicarbonate, without which no complexation occurs [11–13].

The formation of the metallotransferrin results in the development of an intense visible absorption [12] and chemical modification studies as well as UV difference spectral measurements suggest the involvement of 2–3 tyrosinates per metal ion [14–21]. Resonance Raman spectroscopy has provided the definitive evidence for the participation of tyrosinates in the development of the metal chromophore [22–25]. These experiments show four characteristic peaks (Table 1) assigned to phenolate deformations, observed at ca. 1600, 1500, 1270 and 1170  $\text{cm}^{-1}$ . The first two are assigned mainly to C–C ring stretching deformations, the third principally to a C–O stretch, and the last to a C–H bending mode [24]. The data indicate that the C–O stretch is the most sensitive of the four to the changing environment, exhibiting a range from 1248 to 1288  $\text{cm}^{-1}$ , while the others remain within a 10  $\text{cm}^{-1}$  range with few exceptions. Similar vibrations have been observed in the resonance Raman spectra of synthetic iron and copper phenolate complexes [23,24]. Thus, the involvement of tyrosinates in metal coordination in transferrins is unambiguously demonstrated.

The iron transferrins exhibit visible spectra with absorbance maxima near 470 nm. A resonance Raman excitation profile of Fe(III)–serotransferrin exhibits a complex vibronic progression at 1000  $\text{cm}^{-1}$  intervals [23]. This has been ascribed to enhanced scattering from successive excited state vibrational levels involving the phenolate C–O stretching mode. A similarly complex profile is also observed for  $[\text{Fe}(\text{EHPPG})]^-$ , a model complex with two phenolates, two amino groups, and two carboxylates coordinating to the iron [26]. The observation of such complex profiles is quite interesting, though no other metal–tyrosinate system has shown this behavior thus far; it should be noted, however, that only in this study has a detailed investigation with a dye laser been carried out.

The question of how many tyrosinates are coordinated to the metal center in the transferrins has been discussed extensively. Potentiometric titrations show that three protons are released when ferric ion binds to apotransferrin in the presence of bicarbonate [2,5,20]. The number of protons released remains unchanged when oxalate is substituted for bicarbonate, suggesting that bicarbonate does not contribute to the decrease in pH [28]. The involvement of three phenolates in iron binding has been suggested. Studies with cupric ion, on the other hand, show the release of only two protons, indicating the involvement of two phenolates.

Early UV difference spectral studies on metallotransferrins versus the apoproteins indicated two tyrosinates bound per trivalent metal ion and one per divalent metal ion [16,17,28]. These conclusions were based on measurements of  $\Delta\epsilon$  values between the holo- and apoproteins at 245 nm, where a  $\Delta\epsilon$  value of  $10,000 \text{ M}^{-1} \text{ cm}^{-1}$  per tyrosine was used for the change observed at 245 nm. This value was derived from the change in absorbance observed for the ionization of the phenolic proton in *N*-acetyltyrosine. More recent studies [21], however, show that the  $\Delta\epsilon$  values are dependent on metal ion and that better estimates of  $\Delta\epsilon$  can be obtained from studies of the UV difference spectra of metal complexes of EHPG. Indeed, using these values, two tyrosinates are concluded to bind to all transition metals in metallotransferrins. To rationalize the number of protons released upon ferric ion binding, Harris et al. [29] have proposed that two of these are tyrosyl protons and the third arises from the hydrolysis of the iron-bound water (vide infra), a suggestion consistent with the Lewis acidity of the ferric ion.

Studies to determine factors affecting the phenolate-to-iron(III) charge transfer interaction have been reported [30,31]. The first by Ackermann and Hesse [30] showed that increasing the number of coordinated phenolates resulted in a hypsochromic shift. This conclusion was corroborated by Ainscough et al. [31]. In the latter study of iron complexes ranging from  $\text{FeO}_6$  to  $\text{FeO}_2\text{N}_2\text{O}_2'$  coordination types, they also observed that increasing the number of imidazoles resulted in a blue shift in the charge transfer band whereas increased binding strength gave rise to a red shift. They found that the  $\lambda_{\text{max}}$  values observed for the Fe(III)-transferrins were consistent with an iron environment having either two or three coordinated phenolates; the extinction coefficients observed were similarly ambiguous.

Chemical modification experiments have also provided evidence for histidine coordination to the metal [14,32,33]. Dye sensitized photo-oxidation of ovotransferrin shows a minimum of two histidines per metal ion involved in binding, while ethoxyformylation of both ovotransferrin and serotransferrin sets a maximum of two histidines per metal ion [33]. The above data, taken together, suggest that there are two essential histidines for each binding site.

Magnetic resonance studies also provide evidence for histidine coordination [34–36].  $^{14}\text{N}$  superhyperfine splitting is observed in the EPR spectra of Cu(II)-transferrins; the triplet superhyperfine splitting observed corresponds to only one nitrogen [34]. Furthermore, the hybrid dicupric transferrin complex with one anion site occupied by oxalate and the other by carbonate exhibits an unusual superhyperfine splitting of 1:1:2:1:1 due to the overlap of the triplets of the oxalate and the carbonate complexes. This shows that each copper site has one nitrogen ligand. Pulsed EPR experiments on Cu(II)-serotransferrin reveal nuclear modulation effects on the

Cu(II) signal similar to those exhibited by Cu(II) ligated to imidazole, providing direct evidence for its binding to copper [35]. NMR studies on ovotransferrin suggest the participation of four histidines in the coordination of trivalent ions, i.e., two per site [36].

NMR relaxation studies [37,38] also indicate the presence of one water bound to the metal in Fe(III) and Cu(II) serotransferrin and Fe(III), Mn(II), and Mn(III) ovotransferrin. Slow exchange conditions prevail for the iron proteins, while fast exchange conditions are found for the others.

Most intriguing of the metal ligands is bicarbonate, the obligate anion under physiological conditions. In the absence of this anion, the affinity of the apotransferrin for Fe(III) is so low as not to compete successfully with hydrolytic polymerization and nonspecific binding effects [13]. Thus, there is a synergistic binding of metal ion with anion. But is the anion coordinated to the metal? The  $^{13}\text{C}$  NMR spectra of Co(III)-transferrin- $\text{CO}_3$  and Fe(III)-transferrin- $\text{CO}_3$  have been studied using  $^{13}\text{C}$ -carbonate [39,40]. The former is diamagnetic and exhibits a reasonably sharp signal at 169 ppm downfield of  $\text{Me}_4\text{Si}$  for the tightly bound carbonate. The similarity of this shift to that of carbonate rather than bicarbonate suggest that the anion is bound as carbonate. The iron complex, on the other hand, is paramagnetic and no  $^{13}\text{C}$  signal due to bound  $\text{CO}_3^{2-}$  is observed. The absence of a carbonate signal due to broadening by the iron indicates that the carbonate is a maximum of 4.9 Å away from the iron and carbonate coordination to the iron is a distinct possibility. Similar conclusions are derived from spin labeling studies [41].

The carbonate can be substituted with anions having distinct structural and binding requirements [27,42]. For example, oxalate, malonate and maleate exhibit synergistic binding effects, while succinate, fumarate and monocarboxylic acids do not. This suggests that one carboxylate binds at a protein site while the other coordinates to the iron. The carbonate uniquely serves both functions. Other species which exhibit synergistic binding effects include thioglycolate, salicylate, glycine, glyoxylate and glycolate, indicating a requirement for one carboxylate function presumably for the protein site and one Lewis base function for metal binding [27]. The latter suggestion is supported by the optical spectra exhibited by the various iron-transferrin-anion complexes (Fig. 1). The absorbance maxima range from 505 nm for the thioglycolate complex to 410 nm (shoulder) for the glycolate complex (Table 2). Based on these observations, Schlachach and Bates [27] have proposed the model shown in Fig. 2 for the binding of the synergistic anion with iron in transferrin. Direct evidence for the coordination of a carboxylate function to the metal has been provided by pulsed EPR experiments of Cu(II)-transferrin-oxalate [35]. A comparison of the electron spin echoes of the complexes with  $^{12}\text{C}$ -oxalate and  $^{13}\text{C}$ -oxalate clearly shows the presence

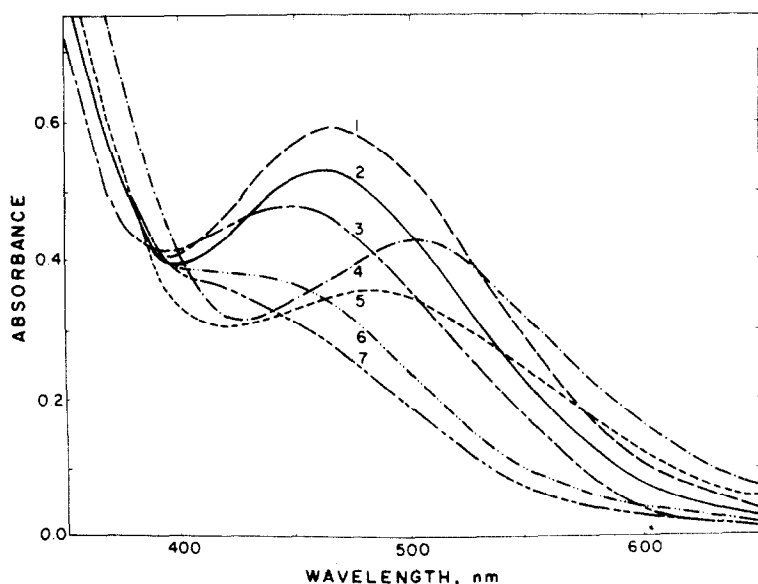


Fig. 1. Visible absorption spectra of Fe(III)-transferrin-anion complexes. The synergistic anions are: (1) nitrilotriacetate; (2) carbonate; (3) salicylate; (4) thioglycolate; (5) glycine; (6) glyoxylate; (7) glycolate. Reprinted with permission from *J. Biol. Chem.*, 250 (1975) 2182-2188.

of a Cu(II)- $^{13}\text{C}$  superhyperfine interaction in the latter complex.

EPR studies on the iron-transferrins have been less informative. The carbonate complexes exhibit signals near  $g = 4.3$ , indicative of a rhombic

TABLE 2

Visible spectra of Fe(III)-transferrin-anion complexes <sup>a</sup>

Anion	Estimated site requirement ( $\text{\AA}$ )	$\lambda_{\text{max}}$ (nm)	$\epsilon$ ( $\text{mM}^{-1} \text{cm}^{-1}$ )
Carbonate	4.6	465	2.60
Oxalate	5.6	465	1.60
Malonate	5.7	465	1.75
Succinate	6.9	No complex formed	
Salicylate	5.9	446	2.40
Glycolate	5.6	410 sh	~1.70
Thioglycolate	6.3	505	2.1
Lactate	5.3	430-440	1.25
Glyoxylate	5.6	430 sh	1.80
Glycine	5.4	488	1.80

<sup>a</sup> Taken from ref. 27.

environment for the high-spin ferric centers [3,42]. The nitrilotriacetate and thioglycolate complexes display similarly rhombic spectra, while the malonate and oxalate complexes exhibit axial spectra [42]. These anions clearly perturb the iron environment, though a more detailed geometrical picture has not emerged. Chasteen [2] has pointed out that the two complexes which exhibit axial EPR spectra also have less intense charge-transfer bands; the decrease in molar extinction coefficient in these complexes is consistent with the more symmetric environment. The values of the zero-field splitting parameter  $D$  for several transferrin complexes have also been measured by obtaining the temperature dependence of the signal at  $g = 4.3$ . Aisen et al. [42] find values of ca.  $0.3 \text{ cm}^{-1}$  for the carbonate complexes of serotransferrin, ovotransferrin, and bovine lactoferrin, while the nitriloacetate complex of serotransferrin exhibits a  $D$  value of  $0.64 \text{ cm}^{-1}$ , double that of the corresponding carbonate complex. The implications of these observations are, however, not yet clear.

Mössbauer studies are in agreement with the EPR determination of  $D$  [43]. The saturation field of  $-550 \text{ kG}$  found for serotransferrin [44] is consistent with an oxygen–nitrogen iron environment and no thiolate coordination [45].

The two metal binding sites in transferrin are distinct; EPR spectra of the Cr(III) [13,25] and  $\text{VO}^{2+}$  [46–48] proteins most clearly exhibit the difference spectroscopically. Chemically, the sites are distinguished by differences in iron affinity. The dissociation of Fe(III) from the protein is biphasic at pHs below 7 [6]. At pH 6.7, the affinities of the two sites for iron differ by more than twenty-fold [49]. Furthermore, the lower affinity site can be selectively occupied with iron if ferric chloride or ferric complexes of oxalate and citrate are used, while the higher affinity site can be preferentially loaded with Fe(III)–nitrilotriacetate [7,49]. The possibility that the two sites may have different functions in the overall scheme of iron transport has been postulated [50] but neither proved nor disproven [2].

The distance between the two metal binding sites has been measured by

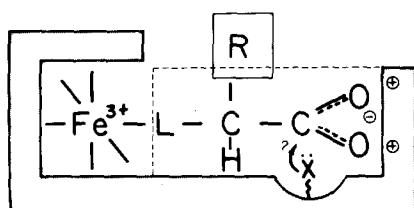
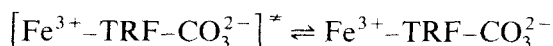
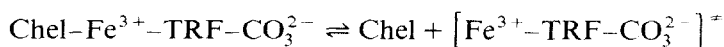
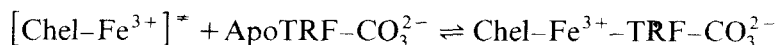
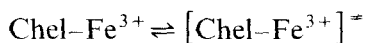
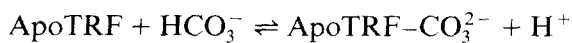


Fig. 2. A model for the binding Fe(III) and the synergistic anion to apotransferrin. Reprinted with permission from J. Biol. Chem., 250 (1975) 2182–2188.

fluorescence techniques, the most recent by observing energy transfer from an excited terbium ion bound at one site and a ferric ion bound at the second site on the same molecule [51]. By measuring the effect of iron on the terbium lifetime, O'Hara et al. [51] have concluded that the intersite distance is  $35.5 \pm 4.5$  Å. This compares with other reports that the two metals are separated by greater than 43 Å (obtained by lifetime measurements) [52] or by  $25 \pm 2$  Å (determined by fluorescence quenching) [53]. All three experiments have inherent uncertainties and the intersite distance will have to be measured by other techniques as well.

Finally, the mechanism for the formation of Fe(III)–transferrin from apotransferrin has been investigated. Bates [54] proposes the following sequence of events:



where TRF and Chel represent transferrin and a chelator, respectively and  $[\text{Chel-Fe}^{3+}]^*$  and  $[\text{Fe}^{3+}\text{-TRF-CO}_3^{2-}]^*$  represent conformational states where the ferric center is partially exposed.

That bicarbonate binds to apoTRF and that this complex acts as the nucleophile for the metal center is indicated by several observations. Most compelling is the  $^{13}\text{C}$  NMR evidence for bicarbonate–apoTRF complex formation [40]. Also indicative is the hyperbolic dependence on  $\text{HCO}_3^-$  of the rate of transferrin formation from apoTRF and a variety of iron complexes as well as the alteration of transferrin reactivity with the substitution of other synergistic anions for bicarbonate [55,56].

Evidence for the quaternary complex has been obtained from stopped-flow kinetic studies [54,57]. The reaction of Fe(III)–acetohydroxamate with apotransferrin– $\text{CO}_3^{2-}$  is clearly biphasic. The first phase requires a few seconds for completion and generates a transient intermediate exhibiting an absorbance maximum at 432 nm, compared to an absorbance maximum of 465 nm for Fe(III)–transferrin– $\text{CO}_3^{2-}$  complex. Similar biphasic kinetics have been observed for the reaction of Fe(III)–nitriloacetate with apotransferrin– $\text{CO}_3^{2-}$ , though the transient spectrum differed from the product spectrum only in molar absorptivity [54,56].



### C. UTEROFERRIN AND PURPLE PHOSPHATASES

In recent years, various investigators have reported the isolation of purple enzymes with phosphatase activity. These are found in mammals [58–66], plants [67–75] and bacteria [76]. The best characterized thus far are uteroferrin from pigs and the acid phosphatases from beef spleen and sweet potato.

Uteroferrin is a basic iron-containing glycoprotein of mol. wt. 40,000 found in the allantoic fluid of midpregnant pigs and the uterine flushings of pseudo-pregnant sows [58–62]. The oxidized protein exhibits a vivid purple color associated with an absorption spectrum with a maximum near 550 nm [59,62,77]. Reducing agents such as ascorbate or  $\beta$ -mercaptoethanol effect a blue shift to 508 nm, rendering the protein pink [59,61,62]; this form exhibits acid phosphatase activity with a pH optimum near pH 4.9. The purple form can be regenerated by treating the pink protein with  $\text{Fe}(\text{CN})_6^{3-}$  or peroxide [59]. The term uteroferrin has been coined by workers who have observed its abundant production during pregnancy. They suggest that this protein may serve as a key supplier of iron for the conceptus [77]; thus uteroferrin by analogy to transferrin. Others, however, believe that this protein functions as a phosphatase *in vivo* [62–64].

Like the transferrins, uteroferrin exhibits resonance Raman spectra with characteristic phenolate deformations (Table 1) [78,79]; this establishes uteroferrin as another member of the emerging class of iron-tyrosinate

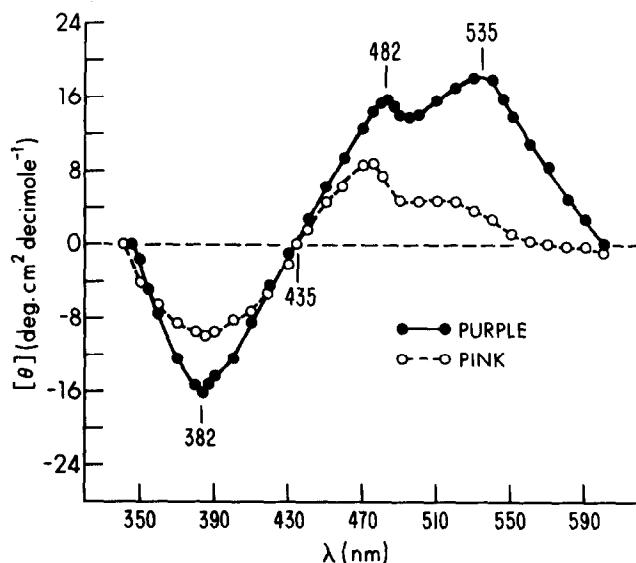


Fig. 3. CD spectra of pink and purple uteroferrin. Reprinted with permission from J. Biol. Chem., 257 (1982) 3766–3770.

proteins [80]. Both purple and pink forms exhibit phenolate modes, the main differences being the  $8\text{ cm}^{-1}$  shift for the  $\nu_{\text{CO}}$  and a broadening of both the  $\nu_{\text{CO}}$  and the  $1600\text{ cm}^{-1}$  features in the pink form. The excitation profile of purple uteroferrin exhibits a maximum near  $550\text{ nm}$  consistent with the visible spectrum [78]. CD spectra, however, reveal several transitions (Fig. 3) [79], which have been interpreted as resulting from three phenolates, one orthogonal to two which act as a pair. The CD maximum at  $535\text{ nm}$  (as well as one at  $305\text{ nm}$ ) is assigned to the charge-transfer interaction of the orthogonal phenolate to the ferric center, while the peaks at  $482$  and  $382\text{ nm}$  result from an exciton-splitting of the charge transfer interactions of the pair of phenolates to the ferric center [79]. This interpretation seems to be in disagreement with the observed excitation profile of purple uteroferrin [78]. The protein would be expected to exhibit maxima near  $540$  and  $480\text{ nm}$  in accordance with the CD maxima and this is clearly not the case. The matter remains to be resolved.

Antanaitis et al. [79] also observe a feature at ca.  $570\text{ cm}^{-1}$  in the resonance Raman spectra of both purple and pink uteroferrin and assign it as arising from vibrations associated with *cis*-coordinated phenolates, by analogy to peaks at  $528\text{ cm}^{-1}$  in  $[\text{Fe}(\text{C}_2\text{O}_4)_3]^{3-}$  and  $535\text{ cm}^{-1}$  in  $[\text{Fe}(\text{cat})_3]^{3-}$  which have been assigned to chelate vibrational modes [81,82]. This assignment, if subsequently confirmed by model compounds, would be most useful in determining coordination environments in the iron-tyrosinate proteins. The transferrins [24] and protococatechuate 3,4-dioxygenase [83,84] all exhibit this feature which is clearly neither an Fe-O stretch nor an internal tyrosine ring mode.

There has been considerable disagreement on the iron content of uteroferrin with reports of one and two gram-atoms of iron per mole of protein [61,62,85]. The irons in the two-iron protein are bound with different affinities [62]. Removal of the more loosely bound metal results in the loss of phosphatase activity, which can be restored by the addition of ferrous ion and mercaptoethanol. The addition of zinc also regenerates phosphatase activity, indicating that an iron-zinc enzyme can be formed. Other properties of this interesting hybrid protein have not been reported.

Early EPR studies on uteroferrin assigned a signal at  $g = 4.3$  to the iron in the protein by analogy to the transferrins [61]; this has subsequently been ascribed to a small amount of adventitiously bound iron [85]. Uteroferrin actually exhibits EPR spectra observable only at liquid helium temperatures (Fig. 4) with  $g_{\text{av}} = 1.74$  [85,86]. All principal  $g$  values are well below the free electron value and this is reminiscent of signals observed for the reduced ferredoxins [87] and the semi-methemerythrins [88] where antiferromagnetic interactions between the irons give rise to the low  $g$  values. This suggests that the active site of uteroferrin may consist of binuclear iron centers. Both

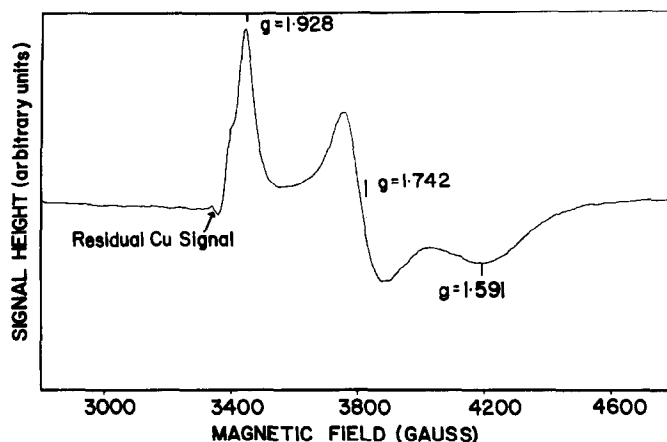


Fig. 4. EPR spectrum of pink uteroferrin. Reprinted with permission from *J. Biol. Chem.*, 255 (1980) 11204–11209.

purple and pink forms have been reported to exhibit this novel EPR signal, whose intensity corresponds to one spin per iron; this now appears to be in error [89a]. Work in progress suggests that the active site in uteroferrin may approach the structure proposed for the beef spleen purple phosphatase (*vide infra*).

The beef spleen acid phosphatase, with a molecular weight of 40,000 and subunits of 15,000 and 24,000 [62,64], exhibits properties similar to uteroferrin. The enzyme as isolated, gives rise to a visible spectrum with a  $\lambda_{\max}$  near 550 nm and an extinction coefficient of ca.  $2000 \text{ M}^{-1} \text{ cm}^{-1}$  [64]. This suggests that the beef spleen acid phosphatase belongs to the class of iron-tyrosinate proteins, and unpublished resonance Raman data indicate this to be so [89b]. Reduction of the enzyme with ascorbate and ferrous ion results in the shift of the  $\lambda_{\max}$  to 505 nm and the elaboration of acid phosphatase activity [62,64].

Two irons are found per mole of enzyme [62,64] and, in agreement with uteroferrin, only a weak EPR signal at  $g = 4.3$  is observed, corresponding to less than 5% of the total iron [64]. Upon reduction, rhombic signals centered at  $g = \text{ca. } 1.77$  are observed; these correspond to one spin per two iron atoms [65]. Addition of phosphate to the EPR-active species results in the disappearance of the signal and the conversion of the pink form to the purple form [66]. Magnetic susceptibility measurements show that the oxidized and reduced proteins are both antiferromagnetically coupled systems ( $-2J \geq 100 \text{ cm}^{-1}$ ), with  $S = 0$  and  $S = 1/2$  ground states, respectively [65]. Thus a binuclear diferric center is proposed for the purple enzyme with a ferric-ferrous pair corresponding to the pink form [65].

As reported for uteroferrin, one of the iron atoms can be replaced by zinc resulting in a ferric-zinc enzyme with full catalytic activity [65]. This form

exhibits a highly temperature dependent EPR signal at  $g = 4.3$  and magnetic susceptibility consistent with a high-spin ferric state. Interestingly, the addition of phosphate dramatically sharpens the signal at  $g = 4.3$  and alters the electron spin relaxation sufficiently to allow quantitation of this signal at liquid nitrogen temperatures (one spin per iron). It thus appears that uteroferrin and the beef spleen phosphatase may constitute a class of binuclear iron proteins with tyrosinate coordination. The nature of the bridging group has yet to be elucidated, though the possibility of a  $\mu$ -oxo bridge, suggested by the similarity of  $J$  values for the phosphatase, oxyhemerythrin and metaquo-hemerythrin [90], is intriguing.

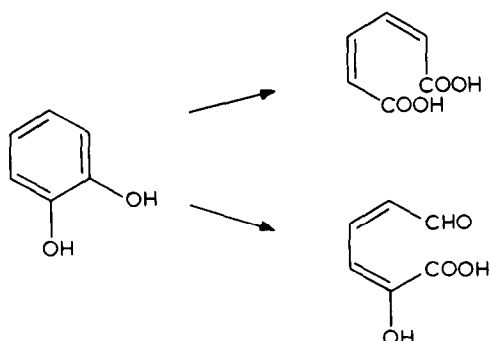
Purple phosphatases from sweet potato [68,69], soybean [70,71], spinach leaves [72] and rice plant cells [73] have also been reported and these contain manganese. The best characterized is the sweet potato enzyme with a molecular weight of 110,000 and one manganese per mole [91]. The enzyme exhibits an absorbance maximum at 515 nm with an extinction coefficient of  $2460 \text{ M}^{-1} \text{ cm}^{-1}$ . This band is assigned to a charge-transfer interaction, which is also consistent with the  $\Delta\epsilon/\epsilon$  ratio obtained from a comparison of the visible and CD spectra. Resonance Raman studies show vibrational modes at 1620, 1508, 1298 and  $1230 \text{ cm}^{-1}$  (though the spectra are inexplicably of poorer quality than those of the iron proteins), consistent with phenolate coordination [91]. Studies on an NBS-treated enzyme (so treated to eliminate tryptophan fluorescence) reveal a peak at  $370 \text{ cm}^{-1}$ , tentatively assigned to a Mn-S stretch [91] by analogy to  $\text{Mn}(\text{Et}_2\text{dtc})_3$  [92]. Sugiura et al. [91] provide evidence for the metal center to be Mn(III) on the basis of the atomic absorption analysis, the visible spectrum, the absence of an EPR signal in the native enzyme and the appearance of an EPR signal due to  $\text{Mn}(\text{H}_2\text{O})_6^{2+}$  when the enzyme is denatured with acid. Though some question has been raised regarding the Mn(III) assignment [64], because of the similarity of the visible spectrum of this enzyme to those of the iron enzymes, it should be noted that Mn(III)-transferrins exhibit visible spectra similar to those of the Fe(III)-transferrins, with absorbance maxima slightly blue shifted with respect to those of the iron proteins [24,25].

One other purple phosphatase deserves mention. This is an extracellular protein from *Micrococcus sodonensis* and has the distinction that it is an alkaline phosphatase and calcium ions stabilize its activity [76]. Indeed, eight calciums are found per 80,000 mol. wt. protein. The purple color is undoubtedly due to a charge-transfer transition and certainly does not arise from a calcium interaction. Analyses of other metals include only copper and zinc, both of which are present only in negligible amounts. The purple color can be eliminated by treatment of the enzyme with EDTA and the loss of activity parallels the loss of color. The apoenzyme can be reconstituted with excess calcium to restore activity but whether the purple color reappears on reconstitution is not clear.

It should be apparent from the above discussion that the purple phosphatases are an interesting new class of enzymes, whose properties remain to be clarified and confirmed. These enzymes are still another example of proteins with redox active metals which catalyze a nonredox process.

#### D. CATECHOL DIOXYGENASES

The catechol dioxygenases are enzymes that catalyze the cleavage of dihydroxybenzene rings, incorporating the elements of molecular oxygen into the product [45,93,94]. Two general reactions are observed:



Those that catalyze reactions resulting in muconic acids are called intradiol dioxygenases, while those that give rise to muconic semialdehydes are extradiol dioxygenases. More is known about the intradiol dioxygenases and these will be discussed first.

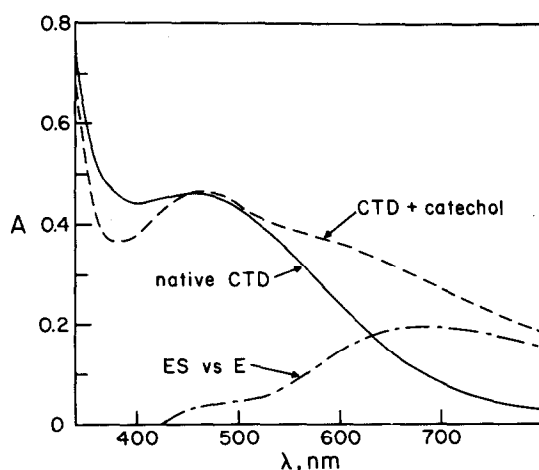


Fig. 5. Visible spectra of native catechol 1,2-dioxygenase and its enzyme-substrate complex in 50 mM Tris-OAc pH 8.5 buffer. Also shown is a difference spectrum between ES and E.

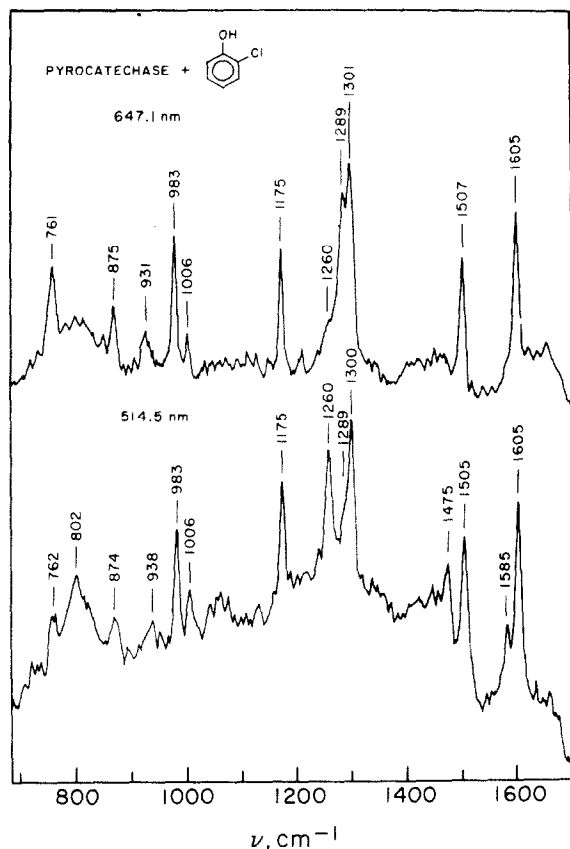


Fig. 6. Resonance Raman spectra of the complex of catechol 1,2-dioxygenase with *o*-chlorophenol using 647.1 and 514.5 nm laser excitation. Reprinted with permission from Biochemistry, 19 (1980) 2588–2593.

### (i) Intradiol dioxygenases

The intradiol dioxygenases, represented by catechol 1,2-dioxygenase and protocatechuate 3,4-dioxygenase, are found only in bacteria; these enzymes are red in color due to the coordination of iron to the polypeptide chain (Fig. 5) [43,93]. Like the transferrins and uteroferrin, resonance Raman studies have shown the presence of tyrosine in the iron coordination environment [80,83,84,95,96]. Further experiments using excitation wavelengths on inhibitor complexes reveal the presence of two distinct tyrosines [97,98] illustrated in Fig. 6. The *o*-chlorophenol complex of catechol 1,2-dioxygenase exhibits three different features in the  $\nu_{\text{CO}}$  region [97]. One at  $1301 \text{ cm}^{-1}$  is assigned to the  $\nu_{\text{CO}}$  of the *o*-chlorophenol by its shift observed when *o*-chlorophenol-4,6- $d_2$  is used. The remaining two features are assigned to

TABLE 3

Mössbauer data on high-spin ferrous proteins

Protein	$\delta(\text{mm s}^{-1})$	$\Delta E_Q(\text{mm s}^{-1})$	Ref.
PCD (reduced)	1.21	3.13	102, 105
CTD (reduced)	1.25	3.14	103
Deoxyhemerythrin	1.20	2.89	106
Rubredoxin (reduced)	0.70	3.25	107
Catechol 2,3-dioxygenase	1.31	3.28	108
Protocatechuate 4,5-dioxygenase	1.28	2.3	104
Protocatechuate 4,5-dioxygenase + substrate	1.28	3.0	104

tyrosinate  $\nu_{\text{CO}}$ 's: they exhibit different excitation profiles, the  $1259\text{ cm}^{-1}$  peak showing maximum intensity near 500 nm and the  $1289\text{ cm}^{-1}$  band peaking near 650 nm. That the other characteristic tyrosinate deformations are not likewise in pairs is not surprising, since these features appear less sensitive to changes in environment than the  $\nu_{\text{CO}}$ . Thus, the C–C stretching deformations of both tyrosines occur at  $1507$  and  $1605\text{ cm}^{-1}$ ; the excitation profiles of these peaks maximize at a wavelength intermediate between 500 and 650 nm. Similar spectral behavior has been observed for the benzoate complex of catechol 1,2-dioxygenase [97] as well as for several complexes of protocatechuate 3,4-dioxygenase (from *Pseudomonas aeruginosa* [98], *Pseudomonas putida* [99] and *Brevibacterium fuscum* [100]). Thus, the coordination of two tyrosinates to the active site iron appears to be a common property of these dioxygenases.

The iron environment in protocatechuate 3,4-dioxygenase from *Pseudomonas aeruginosa* was at first suggested to be like that in rubredoxin (tetrahedral  $\text{Fe}(\text{SR})_4$  coordination) on the basis of EPR data [101]. Both proteins exhibited EPR signals at  $g = 4.3$ , typical of high-spin ferric ions in rhombic symmetry, with the zero field splitting parameter  $D$  for both proteins equal to  $1.6\text{ cm}^{-1}$ . Mössbauer studies on  $^{57}\text{Fe}$ -enriched PCD corroborated the value of  $D$  but the  $H_{\text{sat}}$  value (a measure of the covalency of the iron–ligand bond) was inconsistent with an  $\text{Fe}(\text{SR})_4$  environment [102]. The  $H_{\text{sat}}$  value obtained from Mössbauer data for rubredoxin is  $-410\text{ kG}$ , indicating a fairly covalent environment, while the corresponding value for PCD is  $-525\text{ kG}$ , suggesting an ionic environment. Mössbauer studies on  $^{57}\text{Fe}$ -enriched CTD from *Pseudomonas arvilla* are in general agreement with the above results [103]. The zero field splitting parameter  $D$  is somewhat smaller (ca.  $0.5\text{ cm}^{-1}$ ) and its  $H_{\text{sat}}$  value is  $-530\text{ kG}$ . Thus an  $\text{Fe}(\text{SR})_4$  environment can be definitely ruled out. Indeed, cysteine can be completely

excluded as a ligand since the PCD from *B. fuscum*, which exhibits EPR and Mössbauer parameters similar to those of *Ps. aeruginosa* PCD, contains no cysteine [104].

The iron site in these dioxygenases is thus likely to be an oxygen–nitrogen environment. Mössbauer parameters of reduced PCD [102] and CTD [103] (Table 3) are similar to those of deoxyhemerythrin [106]. The sharpness of the EPR signals from native PCD (*B. fuscum*) have made it possible to demonstrate the presence of one water molecule in the iron coordination sphere [104]. When the enzyme is dissolved in buffer containing 53.7% enriched  $\text{H}_2^{17}\text{O}$ , both signals at  $g = 9.67$  and  $4.27$  are clearly broadened. These observations are also consistent with earlier NMR relaxation studies [109]. The remaining ligands have yet to be elucidated, though histidine would be a very likely possibility because of its ubiquity in metal sites. Thus, the active site of the catechol dioxygenases appears to be similar to that suggested for the transferrins.

Substrate binding effects spectral changes in the dioxygenases. For CTD, the addition of catechol under anaerobic conditions results in the conversion of the pink native enzyme to a blue-gray complex (Fig. 5). The EPR spectra of these complexes reveal high-spin ferric centers with axial distortions and positive zero-field splittings; Mössbauer spectra corroborate these conclusions [101–103]. Resonance Raman studies on enzyme–substrate complexes of PCD and CTD at 647.1 nm exhibit new features which are assigned to the catechol using ring-deuterated substrates [96,110]. At 514.5 nm, both

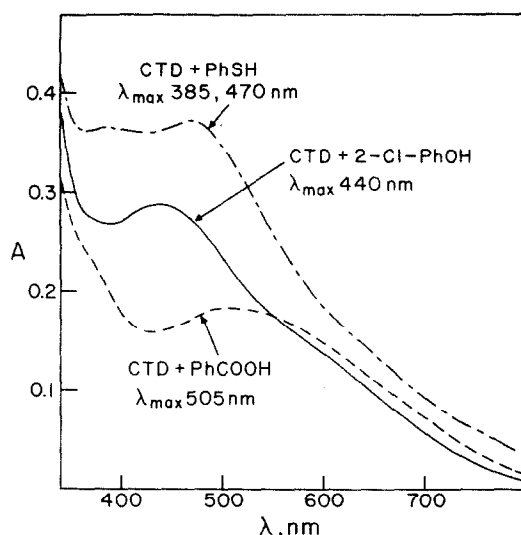


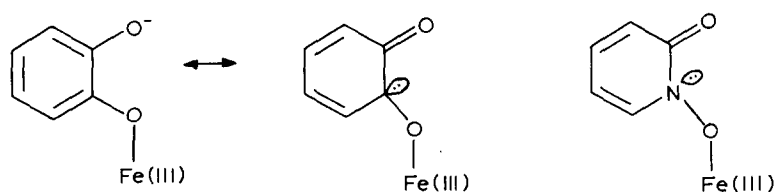
Fig. 7. Visible spectra of catechol 1,2-dioxygenase–inhibitor complexes in 50 mM Tris-OAc pH 8.5 buffer.



catecholate and tyrosinate features are observed, thus demonstrating that the catechol binds to the ferric center without displacing the tyrosines [83,110]. The new features observed at ca. 1260, 1320 and 1480  $\text{cm}^{-1}$  are quite similar to those observed for model catecholate complexes with chelated structures (e.g.  $\text{Fe}(\text{cat})_3^{3-}$ ,  $[\text{Fe}_2(\text{cat})_4\text{OAc}]^{3-}$ ) [82,83,96]. Thus, the substrate has been suggested to chelate to the iron in the ES complex.

Studies with inhibitor complexes, however, are in disagreement with the chelated configuration. The affinities of *m*- and *p*-hydroxybenzoates for PCD have been measured and a consistent preference for the *para* isomer is observed [109]. Resonance Raman studies on the *m*- and *p*-hydroxybenzoate complexes of PCD show conclusively that the *para* hydroxy group coordinates to the iron, while the *meta* hydroxy group does not [98]. These studies thus suggest that the substrate is coordinated in a monodentate configuration in the ES complex. To date, the two conflicting conclusions regarding the mode of substrate binding to the iron have yet to be reconciled.

Another aspect of the substrate binding question is the proposed iron(III)-facilitated ketonization of the bound catecholate [109]

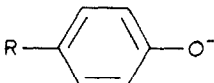


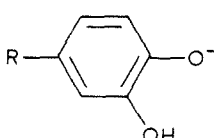
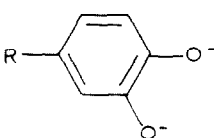


If the proposed tautomerization is favored in the active site, a substrate analogue with the keto structure may be expected to bind tightly to the enzyme. 2-Hydroxyisonicotinic acid *N*-oxide is one such analogue for proto-catechuic acid. The analogue binds so strongly to the PCDs from *B. fuscum*, *Ps. aeruginosa* and *Ps. putida* that only by denaturing the enzymes is the analogue released from the enzymes [104]. The enzyme-analogue complex exhibits a visible spectrum which is blue-shifted and essentially bleached and a sharp EPR spectrum with a large rhombic distortion and a negative zero-field splitting. This complex thus differs markedly from the ES complex. The binding of the analogue to the enzyme is slow (and essentially irreversible) and can be prevented by the presence of substrate. Lipscomb et al. [104] have suggested that the substrate and the analogue may bind to different forms of the enzyme. Oxygen binding triggers a conformational change in the ES complex promoting the formation of the tightly bound ketonized substrate, which then reacts with oxygen. Such a mechanism is rather attractive, but remains to be established.

A variety of other aromatic molecules bind to the active sites of these enzymes, resulting in characteristic spectral changes (Fig. 7). Phenolates

TABLE 4

Absorbance maxima (nm) of Fe(salen)X and corresponding dioxygenase complexes

X	Fe(salen)X <sup>a</sup> (R = H)	CTD-X <sup>b</sup> (R = H)	PCD-X <sup>c</sup> (R = COO <sup>-</sup> )
H <sub>2</sub> O		455	460
	418	440	420
	380, 440	385, 470	
	492	505	525
	418, ~ 590 <sup>d,e</sup>	465, ~ 680 <sup>d,f</sup>	475, ~ 690 <sup>d,f</sup>
	339, 388, 628 <sup>d,g</sup>		

<sup>a</sup> Fe(salen)X data obtained from ref. 112. <sup>b</sup> Catechol 1,2-dioxygenase data obtained from ref. 97. <sup>c</sup> Protocatechuate 3,4-dioxygenase data obtained from ref. 98. <sup>d</sup> Catecholate-to-iron(III) charge transfer interaction. <sup>e</sup> Deduced from Raman excitation profile. <sup>f</sup> Approximated from ES vs. E difference spectrum. <sup>g</sup> Assigned by resonance Raman spectroscopy.

induce blue shifts in the  $\lambda_{\max}$  values, while carboxylates cause red shifts. Thiophenolate coordination results in a significant increase in the enzyme absorbance, indicating perhaps the addition of a new charge-transfer interaction. The spectral data for the various complexes is summarized in Table 4. Resonance Raman spectra of these complexes show that the tyrosinate coordination persists upon inhibitor binding [97,98,110]. Phenolate vibrations are also observed, while thiophenolate and carboxylate modes are not. Carboxylate modes are not expected to be observed, since carboxylate-to-iron charge transfer interactions do not occur in the visible region. Thiolate-to-iron interactions do occur in the visible; however, attempts to obtain spectra at excitation wavelengths other than 647.1 nm result in the conversion of the

orange-brown complex to a purple form upon prolonged irradiation [110].

The binding of the various inhibitors clearly modulates the energy of the phenolate-to-iron charge transfer interaction in the enzymes. The observed changes in the absorbance maxima have been mimicked in a simple model system, based on the tetradentate ligand ethylenebis(salicylideneimine) or salen. Salen provides a coordination environment of two phenolates to model the established two-tyrosinate coordination of the dioxygenases and two imine nitrogens to simulate, albeit crudely, the suggested imidazole coordination. A series of  $\text{Fe(salen)X}$  complexes have been synthesized where X is phenolate, thiophenolate, benzoate and catecholate, and electronic spectra of these are compared with those of corresponding enzyme complexes (Table 4) [111]. The match between the  $\text{Fe(salen)}$  series and the CTD series is particularly encouraging, considering the simplicity of the model system. But we are only beginning to understand how the phenolate-to-iron(III) charge transfer interaction is affected by the other ligands in the complex [112]. Further studies may provide information regarding the geometries of such complexes and the relative configurations of ligands in these complexes.

Two model catecholate complexes with  $[\text{Fe(salen)}]^+$  have been characterized [111,113]. The first is formed by an anaerobic ligand exchange reaction of  $\text{Fe(salen)OAc}$  with excess catechol and has the formulation  $\text{Fe(salen)catH}$ . The presence of the protonated ligand is clear in the IR spectrum exhibiting a sharp  $\nu_{\text{OH}}$  at  $3380\text{ cm}^{-1}$ . The monodentate coordination of the catecholate is unequivocally demonstrated in the crystal structure of the analogous  $\text{Fe(saloph)catH}$  [113]. The catecholate retains its monodentate character in solution as shown by the similarity of its electronic and NMR spectrum to those of phenolate complexes [112].

The second complex is obtained by treatment of  $\text{Fe(salen)catH}$  with KH or potassium t-butoxide. A green solution results and affords large crystals of the  $\text{K}^+[\text{Fe(salen)cat}]^-$  complex. An X-ray crystallographic study shows the catecholate chelated to the iron in a six coordinate structure, somewhat distorted from octahedral geometry [114]. Resonance Raman spectra of both monodentate and chelated catecholate complexes exhibit catecholate modes quite similar to those of the enzyme-substrate complexes [110], so Raman spectra may not permit the distinction between the possible modes of catecholate binding in the enzymes.

An investigation into the oxygen susceptibility of the two complexes has been reported [115].  $\text{Fe(salen)DBcatH}$  reacts readily with  $\text{O}_2$  to yield  $\text{Fe(salen)DBSQ}$ , the result of one-electron oxidation. This reaction is monitored with NMR spectroscopy by observing the disappearance and appearance of various paramagnetically shifted resonances assigned to the catecholate and semiquinone complexes (Fig. 8), respectively. The latter

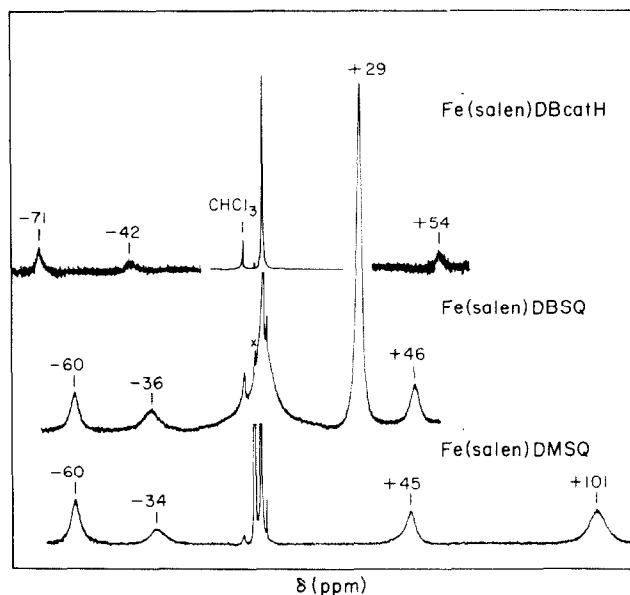


Fig. 8. NMR spectra of Fe(salen)DBcatH, Fe(salen)DBSQ, and Fe(salen)DMSQ. Reprinted with permission from J. Am. Chem. Soc., 103 (1981) 3947–3949.

compound has also been synthesized by Floriani et al. [116] via the oxidative addition of 3,5-di-*t*-butyl-*o*-benzoquinone to Fe(salen) and exhibits the same NMR spectrum as the product of the air oxidation of Fe(salen)DBcatH. [Fe(salen)DBcat]<sup>−</sup>, on the other hand, does not react under these conditions. Indeed, Fe(salen)DBSQ can be reduced by superoxide, affording [Fe(salen)DBcat]<sup>−</sup> and O<sub>2</sub>. Electrochemical studies of [Fe(salen)DBcat]<sup>−</sup> and [Fe(salen)DBSQ] show that the two complexes are interconvertible with an  $E_{1/2}$  of −420 mV vs. SCE. The reduction of DBSQ<sup>−</sup> in aprotic solvent is polarographically observed at −1340 mV [117]. Thus, metal chelation has stabilized the catecholate oxidation state to the extent that the complex is not air-sensitive. These observations on the oxygen reactivity of the catecholate complexes provide a counterpoint to suggestions that the substrate is chelated in the ES complexes. If chelation stabilizes the catecholate state, then the catechol in the ES complex cannot be chelated for the reaction with oxygen to be observed. Further work is in progress.

Numerous mechanistic studies on the intradiol cleaving catechol dioxygenases have been reported. Hayaishi et al. [118] first demonstrated the dioxygenase nature of this reaction with catechol 1,2-dioxygenase catalyzed cleavage of catechol in 1955. Itada subsequently showed that both oxygen atoms incorporated into the muconic acid originated from the same molecule of oxygen [119]. We have recently done the same experiment with PCD and

catechol and arrived at the same conclusions [120]. Thus the mechanism requires the interaction of substrate and oxygen at the active site of the enzyme.

Steady state kinetic studies are consistent with an ordered bimolecular mechanism with substrate binding first [121]. The observation of spectral changes upon substrate binding and the absence of any changes when the native enzyme is under  $O_2$  or  $N_2$  atmosphere are in agreement with this conclusion [122]. One possible mechanism requires the reduction of the ferric center to the ferrous state by substrate, followed by oxygen binding. Indeed, the signal at  $g = 4.3$  of the native enzyme was found to diminish upon substrate binding [122,123]. However, the observed bleaching of the enzyme-substrate complex upon treatment with dithionite and the return of its color with the addition of ferricyanide suggested that substrate binding did not reduce the iron [122]. Subsequent EPR studies at liquid helium temperatures showed that the rhombic signals had been replaced with axial signals [101–103]. Mössbauer studies on the enzyme-substrate complexes of PCD and CTD also find the iron to be high-spin ferric [102,103]. In addition, model studies with catecholates show that they can coordinate to Fe(III) without reducing the iron [112].

Upon exposure to oxygen, the enzyme-substrate complex disappears and product is formed. Fujisawa et al. have reported the spectrum of an oxygenated intermediate generated from PCD, 3,4-dihydroxyphenylpropionate (a slow substrate), and oxygen [124]. The intermediate exhibits a  $\lambda_{\max}$  at 520 nm [124] and has a half-life of about 4 min at 4°C [102]. The decomposition of this intermediate exhibits a first order rate constant comparable to the turnover number of the enzyme acting on the slow substrate [124]. EPR and Mössbauer studies on this species reveal it to be in the high-spin ferric oxidation state [102]. Indeed, this complex was the first enzymatic species unequivocally demonstrated to exhibit a negative zero field splitting. The structural implications of this observation remain to be elucidated. A ferric peroxide complex was suggested as a possible structure for the intermediate [102] but no  $\nu_{O-O}$  has been found in resonance Raman studies [125]. Quenching this complex with acid or urea results in the isolation of starting material and product only; based on these observations, Nakata et al. [126] suggested that this intermediate may be an enzyme-product complex. Indeed, complexes of PCD with dicarboxylates, terephthalate in particular, exhibit absorbance maxima similar to that of the intermediate [98]. Furthermore, pH dependent measurements of the  $K_i$  for terephthalate show a  $pK$  of ca. 8 [98], rather similar to the  $pK$  observed for the pH dependence of the decomposition of the intermediate [127]. At low pH, terephthalate is bound most tightly, while the intermediate has the longest lifetime. It appears then that this intermediate is best designated as EP, rather than  $ESO_2$ .

Oxygenated intermediates have also been found in the reaction of PCD, protocatechuate and oxygen. Initial reports of a single intermediate for this reaction have turned out to be in error [128]; Bull and Ballou found the reported species to consist of several complexes [129–131]. In single turnover stopped-flow studies, the observed rate constant is wavelength dependent, which is inconsistent with the formation of a single species. Visible spectra of two intermediates, designated  $ESO_2$  and  $ESO_2^*$ , can be obtained from stopped-flow experiments at high oxygen pressure (Fig. 9) [131]. These spectra differ markedly from that of the intermediate observed by Fujisawa et al. [124] for PCD, 3,4-dihydroxyphenylpropionate and  $O_2$ . The formation of  $ESO_2$  is oxygen dependent with a second order rate constant of  $5 \times 10^5 \text{ M}^{-1} \text{ sec}^{-1}$  and is apparently irreversible [131].  $ESO_2$  then converts to  $ESO_2^*$  with a first order rate constant of  $450 \text{ sec}^{-1}$ .  $ESO_2^*$  then decays to native enzyme and product at a rate of  $36 \text{ sec}^{-1}$ , consistent with the turnover number of the enzyme.

Parallel experiments with 3,4-dihydroxyphenylpropionate also reveal the presence of two intermediates in this reaction [131], the first resembling  $ESO_2$  and the second resembling the intermediate observed by Fujisawa et al. [124], EP. Thus, changing the substrate alters the kinetic behavior of the various intermediates.

Intermediates have recently been observed for CTD [132]. The reaction of

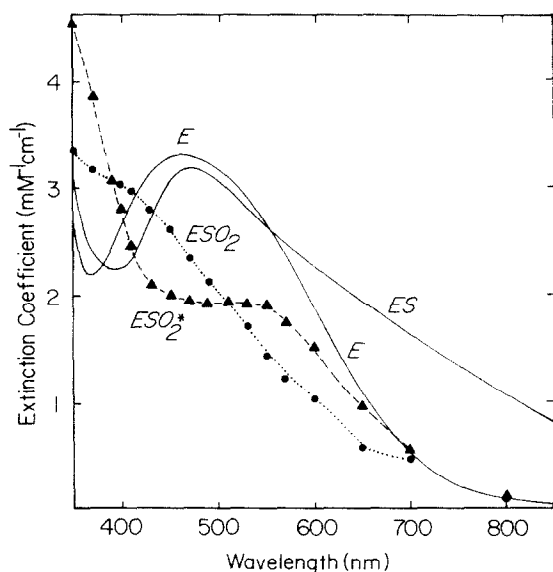


Fig. 9. Visible spectra of protocatechuate 3,4-dioxygenase from *Pseudomonas putida*, its complex with protocatechuate, and intermediates in the reaction of the ES complex with  $O_2$ . Reprinted with permission from J. Biol. Chem., 256 (1981) 12681–12686.

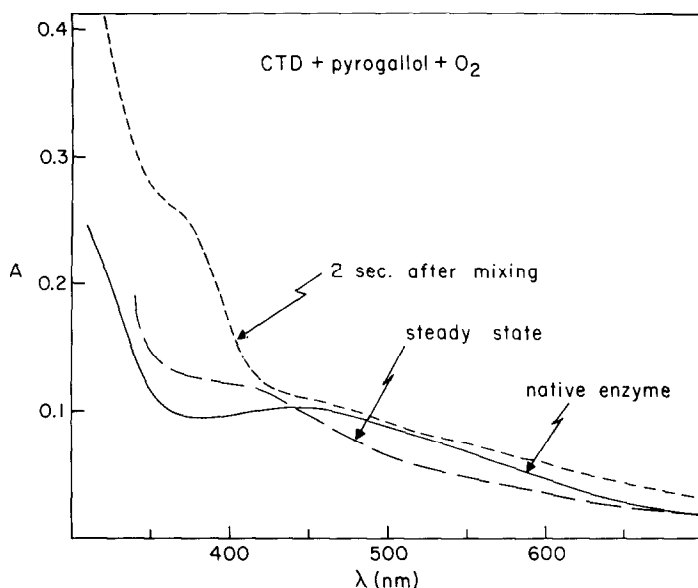


Fig. 10. Visible spectra of catechol 1,2-dioxygenase and intermediates in the reaction of enzyme, pyrogallol and oxygen.

CTD, excess pyrogallol and oxygen results in the observation of two intermediates, **I** and **II**. The visible spectrum of **I** can be approximated by that shown in Fig. 10, which was obtained on a rapid scan spectrophotometer approximately two seconds after the components were mixed. The absorbance near 360 nm is much larger than that of any other CTD complex studies thus far. After a few seconds, this spectrum decays to that of intermediate **II**, which can also be generated under steady state conditions. The spectrum of **II** closely resembles that of  $\text{ESO}_2$  observed by Bull et al. [131] for PCD. This similarity is quite intriguing and serves to emphasize that similar mechanistic pathways are operative in the two dioxygenases.

Intermediate **II** has been further characterized by EPR and Mössbauer spectroscopy [132]. Its EPR spectrum exhibits signals near  $g = 9$  and 4.3. Mössbauer spectra of this intermediate at liquid helium temperatures reveal the generation of a new species with magnetic hyperfine interactions distinct from the native enzyme and the ES complex. Both these observations are consistent with a high-spin ferric center. Since **II** closely resembles  $\text{ESO}_2$  of the PCD sequence,  $\text{ESO}_2$  by inference is also a high-spin ferric complex, which is inconsistent with an earlier suggestion that  $\text{ESO}_2$  may be a ferrous-semiquinone complex [131].

The various stopped-flow kinetic results are summarized in Fig. 11. Thus far, no intradiol dioxygenase complex on the catalytic pathway has been

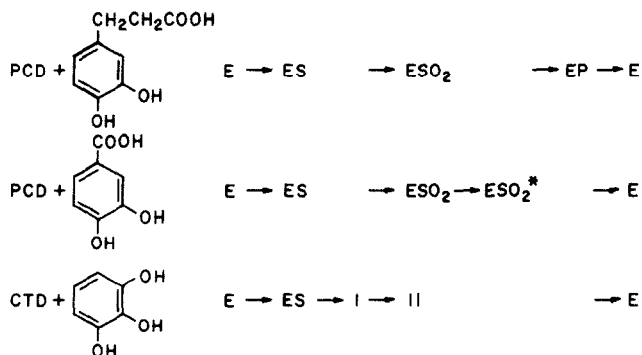


Fig. 11. Summary of stopped-flow kinetic results on the intradiol dioxygenases.

found in the ferrous oxidation state. Early suggestions on the enzyme mechanism favored a scheme wherein the substrate catechol reduced the ferric center and the resulting ferrous center in turn activated  $\text{O}_2$  to effect the ring cleavage.

Que et al. [109] have argued that an alternative mechanism should be considered, given the lack of evidence for a ferrous center in the intermediates studied thus far. The proposed mechanism (Fig. 12) suggests that

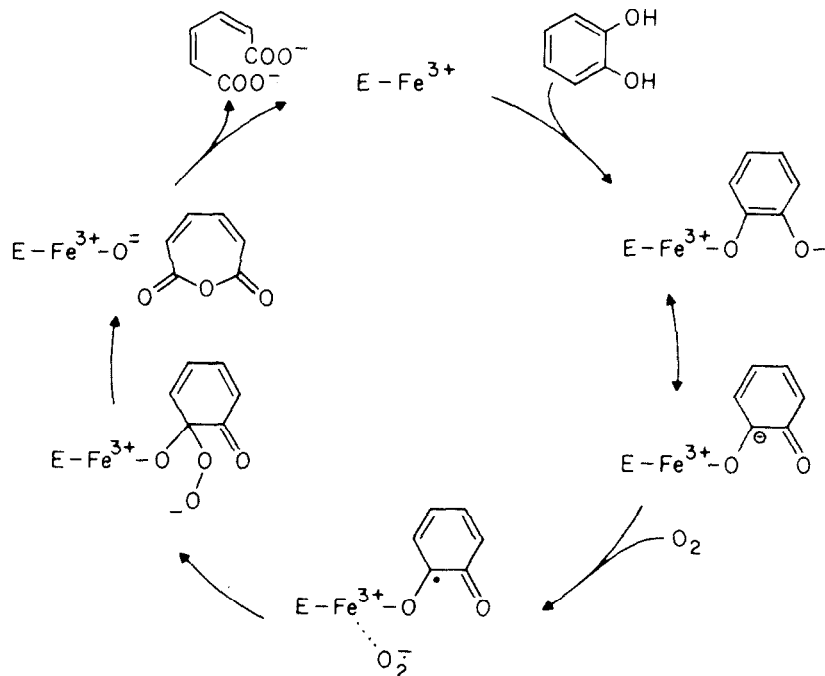


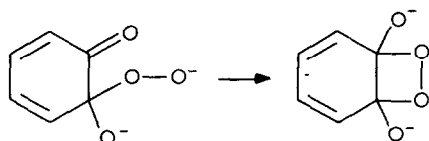
Fig. 12. Proposed mechanism for the intradiol dioxygenases.



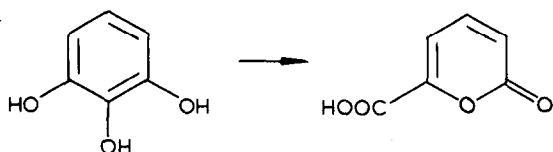
the substrate binds to the iron in a monodentate configuration and loses both its protons. This electron-rich species then transfers one electron to oxygen, generating a ferric-semiquinone-superoxide species. (Catechol dianion generates the semiquinone when exposed to oxygen.) The ferric center can then facilitate the coupling of the two radical species to give rise to the hydroperoxide, which in turn decomposes to product. A similar line of reasoning has also been pursued by Jefford and Cadby [94].

Evidence for any of these intermediates is scant at best. Only the EP complex can be assigned with any certainty. Even in this case, the unique EPR characteristics of the EP complex have yet to be duplicated by an enzyme-carboxylate complex. Evidence for the participation of superoxide in this reaction has been reported [133], but subsequent scrutiny has shown the conclusion to be invalid [134].

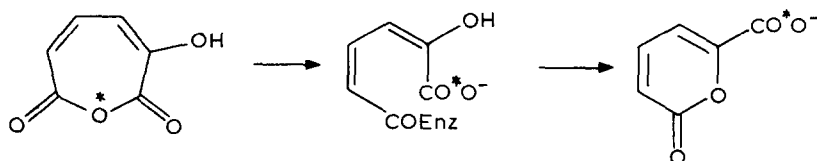
The mechanism we have proposed shows the conversion of the intermediate hydroperoxide to an anhydride, instead of a dioxetane



Hamilton [135] has argued against the dioxetane on thermodynamic grounds, and Saeki et al. [136] has recently provided evidence for the anhydride. Pyrogallol is oxidatively cleaved by PCD to yield 2-pyrone-6-carboxylic acid.



When  $^{18}\text{O}_2$  is used, only the carboxy group is labeled; the other oxygen is lost. The labeling result excludes the possibility that the product arises from the lactonization of the  $\alpha$ -hydroxy-*cis,cis*-muconic acid, since the 2-oxo group of the product would have been half-labeled. The elimination of the muconic acid as an intermediate precludes the dioxetane as an intermediate. The anhydride intermediate can still give rise to product via the mechanism



Muto and Bruice [137] have also presented results on a model system where the peroxide rearrangement pathway is greatly favored over the dioxetane mechanism.

## (ii) Extradiol dioxygenases

The extradiol dioxygenases, though more diverse in their substrate specificities and more abundant than the intradiol enzymes, are much less well-characterized [93]. This is in part due to their greater lability; in many cases, the addition of metal cofactor, usually ferrous ion, into the assay mixture is necessary to obtain maximal activity. Little is known about the coordination about the metal center in these enzymes. They are discussed in this review because the substrate catechol, a special type of phenolate, can in principle, interact with the metal center.

The extradiol dioxygenases are found in bacteria as well as in mammals; substrates for these enzymes include catechols, hydroquinones, and aminophenols. In mammalian systems, these enzymes are represented by homogentisate 1,2-dioxygenase in tyrosine metabolism and 3-hydroxyanthranilate 3,4-dioxygenase in tryptophan metabolism and the biosynthesis of the pyridine nucleotides. The enzymes are typically colorless, with molecular weights of 140,000 consisting of four equivalent subunits. The requirement for ferrous ion has been demonstrated for many enzymes of this type.

Mössbauer studies [108] on catechol 2,3-dioxygenase from *Pseudomonas arvilla* show that the iron is in a high-spin ferrous oxidation state with parameters similar to reduced protocatechuate 3,4-dioxygenase, reduced catechol 1,2-dioxygenase, and deoxyhemerythrin (Table 3), which suggests an oxygen-nitrogen type environment. Furthermore, substrate binding appears not to affect the Mössbauer spectrum.

The situation is more complex with protocatechuate 4,5-dioxygenase from *Pseudomonas testosteroni*. An earlier report [138] concluded that the native enzyme exhibited Mössbauer spectra consistent with either a low spin ferrous ion or a binuclear high-spin ferric pair. Recent studies, however, provide evidence for two distinct iron centers, a high-spin ferrous ion and a high-spin ferric ion [104]. The high-spin ferrous center exhibits Mössbauer parameters  $\delta$  and  $\Delta E_Q$  of 1.28 and 2.3 mm s<sup>-1</sup>, respectively, in the native enzyme; the  $\Delta E_Q$  increases to 3.0 mm s<sup>-1</sup> when substrate is added anaerobically. An NO complex of the enzyme converts the EPR-silent  $S = 2$  species to an  $S = 3/2$  center with  $g$  values at 4.10 and 3.91, thus allowing a convenient method for detecting the Fe(II). The enzyme retains full activity when the NO is removed. Consistent with the Mössbauer results is the observation that the ES complex also reacts with NO, giving rise to a different set of signals.

The high-spin ferric center is observed as a quadrupole doublet in the Mössbauer spectrum at 4.2 K, which indicates that it is either spin-coupled or has a fast electronic spin relaxation rate. Anaerobic addition of substrate results in the development of a signal at  $g = 4.3$ , which approximately

corresponds to one iron per enzyme molecule. It is suggested that substrate binding alters the environment of the EPR-silent ferric center to give rise to this EPR signal. Thus far, no mechanistic insights can be deduced from the present information. It is interesting to note parallels in the observations of Lipscomb et al. [104] with those of Kita et al. [139] on 3,4-dihydroxyphenylacetate 2,3-dioxygenase from *Pseudomonas ovalis*. Kita et al. [139] noted that the native enzyme was EPR-silent and that aerobic substrate addition generated an EPR signal at  $g = 4.3$ . This signal disappeared when  $O_2$  was depleted. They suggested that the iron may cycle through ferrous–ferric oxidation states during turnover, a conclusion which is inconsistent with the data of Lipscomb et al. [104].

Extradiol cleavage activity is also observed for some catechol 1,2-dioxygenases [140–142]. With 3-methyl- and 3-methoxycatechol, both intradiol and extradiol cleavage products are observed; the product ratios observed at room temperature are 17 : 1 and 6 : 1, respectively, with the intradiol product dominant [140]. *o*-Aminophenol, on the other hand, is cleaved solely at the C1–C6 bond yielding an  $\alpha$ -aminomuconic  $\epsilon$ -semialdehyde, which cyclizes to  $\alpha$ -picolinic acid [142]. These observations on a high-spin ferric enzyme indicate that the mechanisms of intradiol and extradiol cleavage may not be so different. However, how one enzyme effects the two cleavage reactions remains to be understood.

A new type of extradiol dioxygenase has recently been recognized [143]. The 3,4-dihydroxyphenylacetate 2,3-dioxygenase from *Bacillus brevis* is a

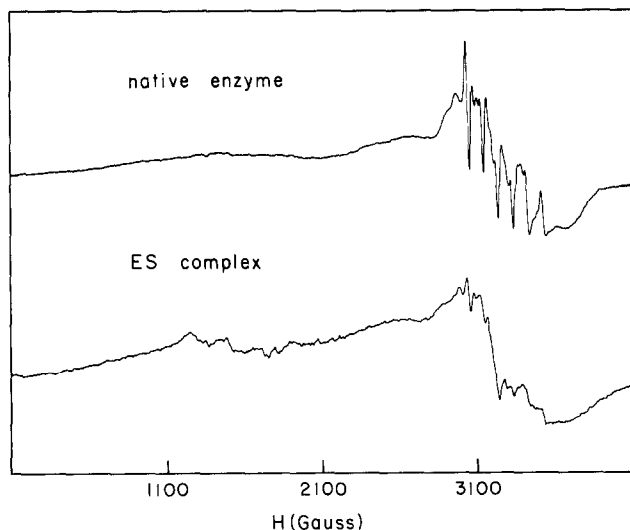


Fig. 13. EPR spectra of 3,4-dihydroxyphenylacetate 2,3-dioxygenase from *Bacillus brevis* and its complex with 3,4-dihydroxyphenylacetate. Reprinted with permission from J. Biol. Chem., 256 (1981) 10941–10944.

manganese(II) containing enzyme. This enzyme catalyzes the same reaction as the enzyme from *Pseudomonas ovalis* [144,145] but, unlike the latter, the former does not require ferrous ion. Indeed, the addition of ferrous ion inhibits enzyme activity. Another important difference is the effect of  $H_2O_2$ . Whereas the *Pseudomonas* enzyme is inactivated by  $H_2O_2$ , the *Bacillus* enzyme is unaffected by it. Similar observations have been made for the iron and manganese superoxide dismutases [146,147].

EPR spectra of the *Bacillus* enzyme show that the metal center is Mn(II) in an environment of low symmetry (Fig. 13). The addition of substrate alters the spectrum indicating some interaction between the manganese center and substrate. Whether this involves a direct coordination is not clear at present. This dioxygenase is the first manganese oxygen-activating enzyme to be found and, so far, the only one; however, it should not be long before more will be found.

Significant progress has been made in the last decade toward the understanding of the structures and mechanisms of the catechol dioxygenases with the application of various spectroscopic and kinetic tools. However, many questions remain unanswered, some of which require the interaction of inorganic, organic and biochemical approaches to provide the complete picture.

#### E. HEME PROTEINS WITH PHENOLATE COORDINATION

To date, two types of heme proteins have been characterized as having phenolate coordination, the mutant hemoglobins [148–150] and catalase [151, 152]. The mutant hemoglobins exhibit iron centers in either the  $\alpha$  or  $\beta$  chains with tyrosine replacing the proximal or distal histidine. As a result, the substituted iron centers are permanently oxidized to Fe(III) in vivo, thereby lowering the oxygen affinity of the protein. Examples of these include HbM Boston ( $\alpha_2^{\text{distal His-58} \rightarrow \text{Tyr}} \beta_2$ ) [148], HbM Iwate ( $\alpha_2^{\text{proximal His-87} \rightarrow \text{Tyr}} \beta_2$ ) [149], HbM Hyde Park ( $\alpha_2 \beta_2^{\text{proximal His-92} \rightarrow \text{Tyr}}$ ) [149] and HbM Saskatoon ( $\alpha_2 \beta_2^{\text{distal His-63} \rightarrow \text{Tyr}}$ ) [150]. The  $\alpha$  chain mutants have abnormally low oxygen affinity which results in cyanosis, an almost absent Bohr effect, and virtually no heme–heme interaction [153–155]. In contrast, the  $\beta$  chain mutants have normal oxygen affinity, a normal Bohr effect, but no cooperativity [156,157]. The effect of the tyrosinate coordination is to render the redox potential of the mutant chains so negative that neither ascorbate nor hemoglobin reductase can reduce the ferric center [148,158]. The coordination of the tyrosinate has been demonstrated in several cases by X-ray crystallography [148,149]. NMR studies on HbM Iwate in solution show non-exchangeable proton resonances ca. 80 ppm downfield from DSS assigned to protons on the

TABLE 5  
EPR data on heme-phenolate complexes

Complex	EPR signals	Ref.
HbM Iwate	6.2, 5.8	161
Boston	6.30, 5.71, 2.00	161
Saskatoon	6.65, 5.35, 2.00	161
Hyde Park	6.27, 5.7, 2.00	161
	7, 5, 2	
Fe(PPIXDBE) (OC <sub>6</sub> H <sub>4</sub> -4-NO <sub>2</sub> )	6.17, 1.97	158
(OC <sub>6</sub> H <sub>3</sub> -3,4-Me <sub>2</sub> )	5.95, 5.07, 1.97	158
[OC <sub>6</sub> H <sub>3</sub> -2,6-(OMe) <sub>2</sub> ]	7.9, 5.12, 2.06	158
[OC <sub>6</sub> H <sub>3</sub> -3,5-(OMe) <sub>2</sub> ]	7.2, 5.17, 2.0	158
Fe(PPIXDBE) (OC <sub>6</sub> H <sub>4</sub> -4-NO <sub>2</sub> )(1-Melm)	2.61, 2.24, 1.86	158
Fe(PPIXDBE) [OC <sub>6</sub> H <sub>3</sub> -2,6-(OMe) <sub>2</sub> ](1-Melm)	2.56, 2.21, 1.85	158
Catalase	6.6, 5.4, 1.99	168

coordinated tyrosinate [159]. The assignment is confirmed by a study on Fe(DPIXDME)(OPh) where *ortho* and *meta* protons are shifted in opposite directions by the paramagnetic center, consistent with a  $\pi$ -delocalization mechanism [160]. (A recent study on iron-phenolate complexes provides further corroboration of the assignments [112].)

Model studies with synthetic iron porphyrin phenolates provide a good comparison with the properties of the mutant hemoglobins [158]. Using [Fe(PPIXDBE)]<sub>2</sub>O, a series of phenolate complexes has been synthesized and found to be high-spin and pentacoordinate. These complexes exhibit visible spectra with  $\alpha$  bands around 600–617 nm depending on the aryl group. This compares well with the 600 nm  $\alpha$  bands observed for HbM Boston [148] and HbM Saskatoon [155]. The synthetic complexes exhibit axial EPR spectra with rhombic distortions similar to those of the mutant hemoglobins [161] (Table 5). Low-spin ferric six-coordinate complexes synthesized by adding 1-methyl-imidazole to the pentacoordinate complexes exhibit EPR signals characteristic of phenolate coordination; however, no mutant hemoglobin has been observed to exhibit such signals. Most interesting is the cyclic voltammetry of Fe(PPIXDBE)OC<sub>6</sub>H<sub>4</sub>-4-NO<sub>2</sub> which shows an  $E_{1/2}$  of –430 mV vs. SCE. This is approximately 200 mV more negative than other types of heme complexes and reflects the effect of phenolate coordination on the iron redox potential.

Catalase, an enzyme found in almost all respiring organisms to protect against the harmful effects of H<sub>2</sub>O<sub>2</sub>, catalyzes the disproportionation of H<sub>2</sub>O<sub>2</sub> to O<sub>2</sub> and H<sub>2</sub>O. The first H<sub>2</sub>O<sub>2</sub> oxidizes the high-spin ferric enzyme by two electrons, generating an intermediate similar to compound I of horse-

radish peroxidase, while the second  $\text{H}_2\text{O}_2$  reduces this intermediate to the native enzyme, evolving  $\text{O}_2$  in the process. Various functional groups have been postulated as axial ligands for the heme groups including carboxylate [162,163], phenolate [164], imidazole [165] and  $\text{OH}^-/\text{H}_2\text{O}$  [163,164,166,167]. Recent X-ray crystallographic studies on beef liver catalase [151,152] have now determined the fifth ligand to be tyrosine with the sixth position vacant, affording a five-coordinate heme phenolate complex as in the mutant hemoglobins. Both EPR [168] and visible spectra [163] of catalase resemble those of the mutant hemoglobins, in agreement with the crystal structure. However, the role of the tyrosine in the chemistry of  $\text{H}_2\text{O}_2$  disproportionation has not yet been elucidated.

#### F. SUMMARY

The involvement of phenolates in the coordination chemistry of metal centers in metalloproteins is now clearly established in several systems. How the presence of this ligand affects the properties of the metal center is an important question to answer. Understanding how the phenolate-to-metal charge transfer interaction is modulated by other ligands in the metal coordination environment will provide insights into the nature of these other ligands and perhaps the coordination geometry as well. The synthesis of inorganic complexes with phenolate coordination and the continued application of physicochemical techniques on both proteins and synthetic analogues should afford answers to many of these questions.

#### ACKNOWLEDGEMENTS

This work was supported by the National Institutes of Health (GM-25422). L.Q. is an Alfred P. Sloan Research Fellow (1982–1984) and the recipient of an NIH Research Career Development Award (1982–1987).

#### NOTE ADDED IN PROOF

Since the completion of this review, several more papers have been published which relate to the coordination chemistry of metalloproteins with phenolate ligands.

With regard to the transferrins, a systematic study of  $\text{Co(III)}$ ,  $\text{Cr(III)}$ ,  $\text{Cu(II)}$ , and  $\text{Mn(III)}$  EHPG complexes has been undertaken for comparison with corresponding metallotransferrins [169]. Both racemic and meso isomers of the complexes have been isolated and the results indicate that EHPG serves as a reasonable model for metal binding in the transferrins.

An EPR study of copper human serotransferrin at 2–4 GHz [170] demon-

strates the utility of going to lower frequency to improve the resolution of superhyperfine splittings when a distribution of spin Hamiltonian parameters is present.  $^{14}\text{N}$  superhyperfine splittings are nicely resolved in this study. An electron spin echo study of copper ovotransferrin [171] shows the coordination of one histidine to the copper in each of the sites. The use of  $^{13}\text{C}$ -oxalate in forming the copper protein complex reveals modulation of the spin echoes by the  $^{13}\text{C}$ , demonstrating the coordination of oxalate to the copper. No effects, however, are observed with  $^{13}\text{C}$ -carbonate. These conclusions are in agreement with those obtained from a similar study on copper human serotransferrin.

Studies on the interaction of phosphate with the purple phosphatase from pig allantoic fluid [172] show that phosphate binds tightly to the inactive oxidized form, in agreement with observations on the beef spleen enzyme [66]. Phosphate binding to the catalytically active reduced porcine enzyme is substantially weaker ( $K_d \sim 6$  mM); it, however, potentiates the conversion of the reduced form to a violet, presumably oxidized, inactive form. The spectral conversion ( $\lambda_{\text{max}}$  510  $\rightarrow$  540 nm) occurs within 10 s, while the phosphatase activity decays with  $t_{1/2} = 51$  min. The detailed interactions of phosphate with the active site remain to be elucidated.

Evidence for histidine ligation in the catechol dioxygenases has been obtained from EXAFS studies on protocatechuate 3,4-dioxygenase [173]. The presence of scattering atoms 3.3 Å from the metal center is ascribed to third shell contributions of imidazole C and N. Two histidines are suggested on the basis of the intensity of this feature. A resonance Raman feature at  $274\text{ cm}^{-1}$  is assigned to a  $\nu_{\text{Fe-N(His)}}$ , consistent with the EXAFS data.

NMR studies of the ES complexes of CTD and PCD with 4-methylcatechol as substrate provide insights into how substrate interacts with the ferric center [174]. Based on the isotropic shifts exhibited by the methyl group of 4-methylcatechol, the substrate is shown to be monodentate in CTD and chelated in PCD. These assignments are consistent with observations on the synthetic catecholate complexes.

Three synthetic systems which effect catechol cleavage have also been reported. They include  $\text{Fe(NTA)}$  in 0.6 M borate buffer pH 8.5 mixed with MeOH or DMF [175],  $\text{RuCl}_2(\text{PPh}_3)_3$  in 1,1,2-trichloroethane [176] and  $\text{VO(salen)}$ ,  $\text{VO(acac)}$  and  $\text{VCl(salen)}$  in dichloromethane [177]. All three systems cleave 3,5-di-*tert*-butylcatechol. The iron system gives rise to lactones, while the other two yield 4,6-di-*tert*-butylmuconic anhydride and 4,6-di-*tert*-butyl-2-pyrone as products.

A study on 2-hydroxyisonicotinic acid *N*-oxide as a transition state analogue for PCD has also been reported [178]. The observations agree with those of Lipscomb et al. [104].

There are also several proteins where tyrosine coordination has been

suggested but which are not covered by this review. These include the binuclear copper proteins, hemocyanin and tyrosinase, where tyrosine is proposed as the bridging ligand in the met forms [179,180], as well as *p*-hydroxyphenylpyruvate dioxygenase [181] which as isolated exhibits a low-spin ferric EPR signal and an intense blue color ( $\lambda_{\text{max}}$  595  $\epsilon$  2600 M<sup>-1</sup> cm<sup>-1</sup>).

## REFERENCES

- 1 P. Aisen and I. Listowsky, *Ann. Rev. Biochem.*, 49 (1980) 357, and references therein.
- 2 N.D. Chasteen, *Coord. Chem. Rev.*, 22 (1977) 1 and references therein.
- 3 R. Aasa, B.G. Malmström, P. Saltman and T. Vänngård, *Biochim. Biophys. Acta*, 75 (1963) 202.
- 4 T.G. Spiro and P. Saltman, *Struct. Bonding (Berlin)*, 6 (1969) 116.
- 5 R.C. Warner and I. Weber, *J. Am. Chem. Soc.*, 75 (1953) 5094.
- 6 J.V. Princiotta and E.J. Zapolski, *Nature (London)*, 255 (1975) 87.
- 7 P. Aisen, A. Liebman and J. Zweier, *J. Biol. Chem.*, 253 (1978) 1930.
- 8 P. Aisen, R. Aasa and A.G. Redfield, *J. Biol. Chem.*, 244 (1969) 4628.
- 9 P.L. Masson and J.F. Heremans, *Eur. J. Biochem.*, 6 (1968) 579.
- 10 E.W. Ainscough, A.M. Brodie and J.E. Plowman, *Inorg. Chim. Acta*, 33 (1979) 149.
- 11 E.M. Price and J.F. Gibson, *Biochem. Biophys. Res. Commun.*, 46 (1972) 646.
- 12 A.L. Schade, R.W. Reinhart and H. Levy, *Arch. Biochem.*, 20 (1949) 170.
- 13 G.W. Bates and M.R. Schlabach, *J. Biol. Chem.*, 250 (1975) 2177.
- 14 W.D. Line, D. Grohlich and A. Bezkorovainy, *Biochemistry*, 6 (1967) 3393.
- 15 S.K. Komatsu and R.E. Feeney, *Biochemistry*, 6 (1967) 1136.
- 16 A.T. Tan and R.C. Woodworth, *Biochemistry*, 8 (1969) 3711.
- 17 B. Teuwissen, P.L. Masson, P. Osinski and J.F. Heremans, *Eur. J. Biochem.*, 31 (1972) 239.
- 18 J.L. Phillips and P. Azari, *Arch. Biochem. Biophys.*, 151 (1972) 445.
- 19 S.S. Leher, *J. Biol. Chem.*, 244 (1969) 3613.
- 20 M.R. Schlabach and G.W. Bates, *J. Biol. Chem.*, 248 (1973) 3228.
- 21 V.L. Pecoraro, W.R. Harris, C.J. Carrano and K.N. Raymond, *Biochemistry*, 20 (1981) 7033.
- 22 P.R. Carey and N.M. Young, *Can. J. Biochem.*, 52 (1974) 273.
- 23 B.P. Gaber, V. Miskowski and T.G. Spiro, *J. Am. Chem. Soc.*, 96 (1974) 6868.
- 24 Y. Tomimatsu, S. Kint and J.R. Scherer, *Biochemistry*, 15 (1976) 4918.
- 25 E.W. Ainscough, A.M. Brodie, J.E. Plowman, S.J. Bloor, J.S. Loehr and T.M. Loehr, *Biochemistry*, 19 (1980) 4072.
- 26 N.A. Bailey, D. Cummins, E.D. McKenzie and J.M. Worthington, *Inorg. Chim. Acta*, 18 (1976) L13.
- 27 M.R. Schlabach and G.W. Bates, *J. Biol. Chem.*, 250 (1975) 2182.
- 28 M.H. Gelb and D.C. Harris, *Arch. Biochem. Biophys.*, 200 (1980) 93.
- 29 W.R. Harris, C.J. Carrano, V.L. Pecoraro and K.N. Raymond, *J. Am. Chem. Soc.*, 103 (1981) 2231.
- 30 G.A. Ackermann and D. Hesse, *Z. Anorg. Allg. Chem.*, 375 (1970) 77.
- 31 E.W. Ainscough, A.W. Brodie, J.E. Plowman, K.L. Brown, A.W. Addison and A.R. Ginsford, *Inorg. Chem.*, 19 (1980) 3655.
- 32 M.A. Krysteva, J. Mazurier, G. Spik and J. Montreuil, *FEBS Lett.*, 56 (1975) 337.
- 33 T.B. Rogers, R.A. Gold and R.E. Feeney, *Biochemistry*, 16 (1977) 2299.
- 34 J.L. Zweier and P. Aisen, *J. Biol. Chem.*, 252 (1977) 6090.
- 35 J.L. Zweier, P. Aisen, J. Peisach and W.B. Mims, *J. Biol. Chem.*, 254 (1979) 3512.



- 36 B.M. Alsaadi, R.J.P. Williams and R.C. Woodworth, *J. Inorg. Biochem.*, 15 (1981) 1.
- 37 S.H. Koenig and W.E. Schillinger, *J. Biol. Chem.*, 244 (1969) 6520.
- 38 J.J. Villafranca, R.P. Pillai and R.C. Woodworth, *J. Inorg. Biochem.*, 6 (1976) 233.
- 39 D.C. Harris, G.A. Gray and P. Aisen, *J. Biol. Chem.*, 249 (1974) 5261.
- 40 J.L. Zweier, J.B. Wooten and J.S. Cohen, *Biochemistry*, 20 (1981) 3505.
- 41 R.C. Najarian, D.C. Harris and P. Aisen, *J. Biol. Chem.*, 253 (1978) 38.
- 42 P. Aisen, R.A. Pinkowitz and A. Liebman, *Ann. N.Y. Acad. Sci. U.S.A.*, 222 (1973) 337.
- 43 C.P. Tsang, L. Bogner and A.J.F. Boyle, *J. Chem. Phys.*, 65 (1976) 4584.
- 44 K. Spartalian and W.T. Oosterhuis, *J. Chem. Phys.*, 59 (1973) 617.
- 45 L. Que, Jr., *Struct. Bonding (Berlin)*, 40 (1980) 39.
- 46 J.C. Cannon and N.D. Chasteen, *Biochemistry*, 14 (1975) 4573.
- 47 R.F. Campbell and N.D. Chasteen, *J. Biol. Chem.*, 252 (1977) 5996.
- 48 N.D. Chasteen, L.K. White and R.F. Campbell, *Biochemistry*, 16 (1977) 363.
- 49 R.W. Evans and J. Williams, *Biochem. J.*, 173 (1978) 543.
- 50 J. Fletcher and E.R. Huehns, *Nature (London)*, 218 (1968) 1211.
- 51 P. O'Hara, S.M. Yeh, C.F. Meares and R. Bersohn, *Biochemistry*, 20 (1981) 4704.
- 52 C.K. Luk, *Biochemistry*, 10 (1971) 2838.
- 53 C.F. Meares and J.E. Ledbetter, *Biochemistry*, 16 (1977) 5178.
- 54 R.E. Cowart, N. Kojima and G.W. Bates, *J. Biol. Chem.*, 257 (1982) 7560.
- 55 N. Kojima and G.W. Bates, *J. Biol. Chem.*, 256 (1981) 12034.
- 56 G.W. Bates and J. Wernicke, *J. Biol. Chem.*, 246 (1971) 3679.
- 57 G.W. Bates, unpublished observations, 1981.
- 58 T.T. Chen, F.W. Bazer, J.J. Cetorelli, W.E. Pollard and R.M. Roberts, *J. Biol. Chem.*, 248 (1973) 8560.
- 59 D.C. Schlosnagle, F.W. Bazer, J.C.M. Tsibris and R.M. Roberts, *J. Biol. Chem.*, 249 (1974) 7574.
- 60 F.W. Bazer, T.T. Chen, J.S. Knight, D.C. Schlosnagle, N.J. Baldwin and R.M. Roberts, *J. Anim. Sci.*, 41 (1975) 1112.
- 61 D.C. Schlosnagle, E.G. Sander, F.W. Bazer and R.M. Roberts, *J. Biol. Chem.*, 251 (1976) 4680.
- 62 H.D. Campbell, D.A. Dionysius, D.T. Keough, B.E. Wilson, J. de Jersey and B. Zerner, *Biochem. Biophys. Res. Commun.*, 82 (1978) 615.
- 63 D.T. Keough, D.A. Dionysius, J. de Jersey and B. Zerner, *Biochem. Biophys. Res. Commun.*, 94 (1980) 600.
- 64 J.C. Davis, S.S. Lin and B.A. Averill, *Biochemistry*, 20 (1981) 4062.
- 65 J.C. Davis and B.A. Averill, *Proc. Natl. Acad. Sci. U.S.A.*, 79 (1982) 4623.
- 66 B.C. Antanaitis and P. Aisen, *J. Biol. Chem.*, 257 (1982) 5330.
- 67 S. Nochumson, J.J. O'Rangers and N.V. Dimitrov, *Fed. Proc. Fed. Am. Soc. Exp. Biol.*, 33 (1974) 1378.
- 68 K. Uehara, S. Fujimoto and T. Taniguchi, *J. Biochem.*, 70 (1971) 183.
- 69 K. Uehara, S. Fujimoto and T. Taniguchi, *J. Biochem.*, 75 (1974) 627, 639.
- 70 S. Fujimoto, T. Nakagawa and A. Ohara, *Agric. Biol. Chem.*, 41 (1977) 599.
- 71 S. Fujimoto, T. Nakagawa and A. Ohara, *Chem. Pharm. Bull.*, 25 (1977) 3283.
- 72 S. Fujimoto, T. Nakagawa and A. Ohara, *Chem. Pharm. Bull.*, 25 (1977) 1459.
- 73 I. Igaue, H. Watabe, K. Takahashi, M. Takekoshi and A. Morota, *Agric. Biol. Chem.*, 40 (1976) 823.
- 74 M.M. Jacobs, J.F. Nyc and D.M. Brown, *J. Biol. Chem.*, 246 (1971) 1419.
- 75 W.N. Arnold and R.G. Garrison, *J. Biol. Chem.*, 254 (1979) 4919.
- 76 R.H. Glew and E.C. Heath, *J. Biol. Chem.*, 246 (1971) 1556.
- 77 R.M. Roberts and F.W. Bazer, in W. Beato (Ed.), *Steroid Induced Uterine Proteins*, Elsevier, Amsterdam, 1980, pp. 133-149.

- 78 B.P. Gaber, J.P. Sheridan, F.W. Bazer and R.M. Roberts, *J. Biol. Chem.*, 254 (1979) 8340.
- 79 B.C. Antanaitis, T. Strekas and P. Aisen, *J. Biol. Chem.*, 257 (1982) 3766.
- 80 W.E. Keyes, T.M. Loehr and M.L. Taylor, *Biochem. Biophys. Res. Commun.*, 83 (1978) 941.
- 81 K. Nakamoto, *Infrared Spectra of Inorganic and Coordination Compounds*, Wiley-Interscience, New York, 1970, p. 245.
- 82 S. Salama, J.D. Stong, J.B. Neilands and T.G. Spiro, *Biochemistry*, 17 (1978) 3781.
- 83 R.H. Felton, L.D. Cheung, R.S. Phillips and S.W. May, *Biochem. Biophys. Res. Commun.*, 85 (1978) 844.
- 84 C. Bull, D.P. Ballou and I. Salmeen, *Biochem. Biophys. Res. Commun.*, 87 (1979) 836.
- 85 B.C. Antanaitis, P. Aisen, H.R. Lilienthal, R.M. Roberts and F.W. Bazer, *J. Biol. Chem.*, 255 (1980) 11204.
- 86 B.C. Antanaitis and P. Aisen, *J. Biol. Chem.*, 257 (1982) 1855.
- 87 H. Brintzinger, G. Palmer and R.H. Sands, *Proc. Natl. Acad. Sci. U.S.A.*, 55 (1966) 397.
- 88 B.B. Muhoberac, D.C. Wharton, L.M. Babcock, P.C. Harrington and R.G. Wilkins, *Biochim. Biophys. Acta*, 626 (1980) 337.
- 89a P. Aisen, private communication, 1982.
- b B.A. Averill, private communication, 1982.
- 90 J.W. Dawson, H.B. Gray, N.E. Hoening, G.R. Rossman, J.J. Schreder and R.H. Wang, *Biochemistry*, 11 (1972) 461.
- 91 Y. Sugiura, H. Kawabe, H. Tanaka, S. Fujimoto and A. Ohara, *J. Am. Chem. Soc.*, 103 (1981) 963. Y. Sugiura, H. Kawabe and H. Tanaka, *J. Am. Chem. Soc.*, 102 (1980) 6581. Y. Sugiura, H. Kawabe, H. Tanaka, S. Fujimoto and A. Ohara, *J. Biol. Chem.*, 256 (1981) 10664.
- 92 P.C. Healy and A.H. White, *J. Chem. Soc., Dalton Trans.*, (1972) 1883.
- 93 M. Nozaki, *Topics Curr. Chem.*, 78 (1979) 145.
- 94 C.W. Jefford and P.A. Cadby, *Fortschr. Chem. Org. Naturst.*, 40 (1981) 191.
- 95 Y. Tatsuno, Y. Saeki, M. Iwaki, T. Yagi, M. Nozaki, T. Kitagawa and S. Otsuka, *J. Am. Chem. Soc.*, 100 (1978) 4614.
- 96 L. Que, Jr. and R.H. Heistand, II, *J. Am. Chem. Soc.*, 101 (1979) 2219.
- 97 L. Que, Jr., R.H. Heistand, II, R. Mayer and A.L. Roe, *Biochemistry*, 19 (1980) 2588.
- 98 L. Que, Jr. and R.M. Epstein, *Biochemistry* 20 (1981) 2545.
- 99 T.E. Walsh, D.P. Ballou, A.L. Roe and L. Que, Jr., unpublished results, 1981.
- 100 J.W. Whittaker, J.D. Lipscomb, A.L. Roe and L. Que, Jr., unpublished results, 1981.
- 101 W.E. Blumberg and J. Peisach, *Ann. N.Y. Acad. Sci.*, 222 (1973) 539.
- 102 L. Que, Jr., J.D. Lipscomb, R. Zimmermann, E. Münck, N.R. Orme-Johnson and W.H. Orme-Johnson, *Biochim. Biophys. Acta*, 452 (1976) 320.
- 103 T. Kent, E. Münck, J. Widom and L. Que, Jr., unpublished results, 1981.
- 104 J.D. Lipscomb, J.W. Whittaker and D.M. Arciero, in M. Nozaki, Y. Ishimura and S. Yamamoto (Eds.), *Oxygenases and Oxygen Metabolism*, Academic Press, New York, 1982, pp. 27–38.
- 105 R. Zimmermann, B.H. Huynh, E. Münck and J.D. Lipscomb, *J. Chem. Phys.*, 69 (1978) 5463.
- 106 M.Y. Okamura, I.M. Klotz, C.E. Johnson, M.R.C. Winter and R.J.P. Williams, *Biochemistry*, 8 (1969) 1951.
- 107 P.G. Debrunner, E. Münck, L. Que, Jr. and C.E. Schulz, in W.E. Lovenberg (Ed.), *Iron-Sulfur Proteins Vol. 3*, Academic Press, New York, 1977, pp. 381–417.
- 108 Y. Tatsuno, Y. Saeki, M. Nozaki, S. Otsuka and Y. Maeda, *FEBS Lett.*, 112 (1980) 83.
- 109 L. Que, Jr., J.D. Lipscomb, E. Münck and J.M. Wood, *Biochim. Biophys. Acta*, 485 (1977) 60.
- 110 A.L. Roe and L. Que, Jr., unpublished results, 1982.

- 111 R.H. Heistand II, R.B. Lauffer, E. Fikrig and L. Que, Jr., *J. Am. Chem. Soc.*, 104 (1982) 2789.
- 112 E.W. Ainscough, A.W. Brodie, J.E. Plowman, K.L. Brown, A.W. Addison and A.R. Gainsford, *Inorg. Chem.*, 19 (1980) 3655.
- 113 R.H. Heistand II, A.L. Roe and L. Que, Jr., *Inorg. Chem.*, 21 (1982) 676.
- 114 R.B. Lauffer, R.H. Heistand II and L. Que, Jr., *Inorg. Chem.*, 22 (1983) 50.
- 115 R.B. Lauffer, R.H. Heistand II and L. Que, Jr., *J. Am. Chem. Soc.*, 103 (1981) 3947.
- 116 C. Floriani, G. Fachinetti and F. Calderazzo, *J. Chem. Soc., Dalton Trans.*, (1973) 765.
- 117 E.J. Nanni, Jr., M.D. Stallings and D.T. Sawyer, *J. Am. Chem. Soc.*, 102 (1980) 4481.
- 118 O. Hayaishi, M. Katagiri and S. Rothberg, *J. Am. Chem. Soc.*, 77 (1955) 5450.
- 119 N. Itada, *Biochem. Biophys. Res. Commun.*, 20 (1965) 149.
- 120 F.N. Muralidharan and L. Que, Jr., unpublished observations, 1980.
- 121 M. Nozaki, T. Nakazawa, H. Fujisawa, S. Katani, Y. Kojima and O. Hayaishi, *Adv. Chem. Ser.*, 77 (1968) 242.
- 122 H. Fujisawa, M. Uyeda, Y. Kojima, M. Nozaki and O. Hayaishi, *J. Biol. Chem.*, 247 (1972) 4414.
- 123 T. Nakazawa, M. Nozaki, O. Hayaishi and T. Yamano, *J. Biol. Chem.*, 244 (1969) 119.
- 124 H. Fujisawa, K. Hiromi, M. Uyeda, S. Okuno, M. Nozaki and O. Hayaishi, *J. Biol. Chem.*, 247 (1972) 4422.
- 125 W.E. Keyes, T.M. Loehr, M.L. Taylor and J.S. Loehr, *Biochem. Biophys. Res. Commun.*, 89 (1979) 420.
- 126 H. Nakata, T. Yamauchi and H. Fujisawa, *Biochim. Biophys. Acta*, 527 (1978) 171.
- 127 S.W. May and R.S. Phillips, *Biochemistry*, 18 (1979) 5933.
- 128 H. Fujisawa, K. Hiromi, M. Uyeda, M. Nozaki and O. Hayaishi, *J. Biol. Chem.*, 246 (1971) 2320.
- 129 D.P. Ballou and C. Bull, in W. Caughey (Ed.), *Biochemical and Clinical Aspects of Oxygen*, Academic Press, New York, 1979, pp. 573-587.
- 130 C. Bull and D.P. Ballou, *J. Biol. Chem.*, 256 (1981) 12673.
- 131 C. Bull, D.P. Ballou and S. Otsuka, *J. Biol. Chem.*, 256 (1981) 12681.
- 132 L. Que, Jr. and R. Mayer, *J. Am. Chem. Soc.*, 104 (1982) 875.
- 133 R. Mayer, J. Widom and L. Que, Jr., *Biochem. Biophys. Res. Commun.*, 92 (1980) 285.
- 134 T.E. Walsh and D.P. Ballou, unpublished results, 1980.
- 135 G.A. Hamilton, in O. Hayaishi (Ed.), *Molecular Mechanisms of Oxygen Activation*, Academic Press, New York, 1974, p. 405.
- 136 Y. Saeki, M. Nozaki and S. Senoh, *J. Biol. Chem.*, 255 (1980) 8465.
- 137 S. Muto and T.C. Bruice, *J. Am. Chem. Soc.*, 102 (1980) 7379.
- 138 R. Zabinski, E. Münck, P.M. Champion and J.M. Wood, *Biochemistry*, 11 (1972) 3212.
- 139 H. Kita, Y. Miyake, M. Kamimoto, S. Senoh and T. Yamano, *J. Biochem.*, 66 (1969) 45.
- 140 M. Fujiwara, L.A. Golovleva, Y. Saeki, M. Nozaki and O. Nayaishi, *J. Biol. Chem.*, 250 (1975) 4848.
- 141 C.T. Hou, R. Patel and M.O. Lillard, *Appl. Environ. Microbiol.*, 33 (1977) 725.
- 142 L. Que, Jr., *Biochem. Biophys. Res. Commun.*, 84 (1978) 123.
- 143 L. Que, Jr., J. Widom and R.L. Crawford, *J. Biol. Chem.*, 256 (1981) 10941.
- 144 H. Kita, *J. Biochem.*, 58 (1965) 116.
- 145 M. Ono-Kamimoto, *J. Biochem.*, 74 (1973) 1049.
- 146 K. Asada, K. Yoshikawa, M. Takahashi, Y. Maeda and K. Enmanji, *J. Biol. Chem.*, 250 (1975) 2801.
- 147 J. Lumsden, R. Cammack and D.O. Hall, *Biochim. Biophys. Acta*, 438 (1976) 380.
- 148 P.D. Pulsinelli, M.F. Perutz and R.L. Nagel, *Proc. Natl. Acad. Sci. U.S.A.*, 70 (1973) 3870.
- 149 J. Greer, *J. Mol. Biol.*, 59 (1971) 107.
- 150 P.S. Gerald and M.L. Efron, *Proc. Natl. Acad. Sci. U.S.A.*, 47 (1961) 1758.

- 151 T.C. Reid, III, M.R.N. Murthy, A. Sicignano, N. Tanaka, W.D.L. Musick and M.G. Rossmann, *Proc. Natl. Acad. Sci. U.S.A.*, 78 (1981) 4767.
- 152 M.R.N. Murthy, T.J. Reid, III, A. Sicignano, N. Tanaka and M.G. Rossmann, *J. Mol. Biol.*, 152 (1981) 465.
- 153 T. Suzuki, A. Hayashi, Y. Yamamura, Y. Enoki and I. Tyuma, *Biochem. Biophys. Res. Commun.*, 19 (1965) 691.
- 154 N. Hayashi, Y. Motokawa and G. Kikuchi, *J. Biol. Chem.*, 241 (1966) 79.
- 155 H.F. Bunn, B.G. Forget and H.M. Ranney, *Human Hemoglobins*, W.B. Saunders, Philadelphia, 1977, pp. 336–345.
- 156 H.M. Ranney, R.L. Nagel, P. Hellor and L. Udem, *Biochim. Biophys. Acta*, 160 (1968) 112.
- 157 T. Suzuki, A. Hayashi, A. Shimizu and Y. Yamamura, *Biochim. Biophys. Acta*, 127 (1966) 280.
- 158 E.W. Ainscough, A.W. Addison, D. Dolphin and B.R. James, *J. Am. Chem. Soc.*, 100 (1978) 7585.
- 159 G.N. LaMar, K. Nagai, T. Jue, D.L. Budd, K. Gersonde, H. Sick, T. Kagimoto, A. Hayashi and F. Taketas, *Biochem. Biophys. Res. Commun.*, 96 (1980) 1172.
- 160 W.S. Caughey and L.F. Johnson, *J. Chem. Soc. Chem. Commun.*, (1969) 1362.
- 161 A. Hayashi, T. Suzuki, A. Shimizu, H. Morimoto and H. Watari, *Biochim. Biophys. Acta* 147 (1967) 407.
- 162 H. Theorell, *Adv. Enzymol.*, 7 (1947) 265.
- 163 A.S. Brill and R.J.P. Williams, *Biochem. J.*, 78 (1961) 246.
- 164 P. Nicholls, *Biochim. Biophys. Acta*, 60 (1962) 217.
- 165 A.S. Brill and H.E. Sandberg, *Biophys. J.*, 8 (1968) 669.
- 166 B. Chance, *J. Biol. Chem.*, 194 (1952) 483.
- 167 A. Lanir and A. Schejter, *FEBS Lett.*, 55 (1975) 254.
- 168 K. Torii, T. Iizuka and Y. Ogura, *J. Biochem.*, 68 (1970) 837.
- 169 M.G. Patch, K.P. Simolo and C.J. Carrano, *Inorg. Chem.*, 21 (1982) 2972.
- 170 W. Froncisz and P. Aisen, *Biochim. Biophys. Acta*, 700 (1982) 55.
- 171 J.L. Zweier, J. Peisach and W.B. Mims, *J. Biol. Chem.*, 257 (1982) 10314.
- 172 D.T. Keough, J.L. Beck, J. de Jersey and B. Zerner, *Biochem. Biophys. Res. Commun.*, 108 (1982) 1643.
- 173 R.H. Felton, W.L. Barrow, S.W. May, A.L. Sowell, S. Goel, G. Bunker and E.A. Stern, *J. Am. Chem. Soc.*, 104 (1982) 6132.
- 174 R.B. Lauffer and L. Que, Jr., *J. Am. Chem. Soc.*, 104 (1982) 7324.
- 175 M.G. Weller and U. Weser, *J. Am. Chem. Soc.*, 104 (1982) 3752.
- 176 M. Matsumoto and K. Kuroda, *J. Am. Chem. Soc.*, 104 (1982) 1433.
- 177 Y. Tatsuno, M. Tatsuda and S. Otsuka, *J. Chem. Soc., Chem. Commun.* (1982) 1100.
- 178 S.W. May, C.D. Oldham, P.W. Mueller, S.R. Padgett and A.L. Sowell, *J. Biol. Chem.* 257 (1982) 12746.
- 179 R.S. Himmelwright, N.C. Eickman and E.I. Solomon, *J. Am. Chem. Soc.*, 101 (1979) 1576.
- 180 R.S. Himmelwright, N.C. Eickman, C.D. LuBien, K. Lerch and E.I. Solomon, *J. Am. Chem. Soc.*, 102 (1980) 7339.
- 181 S. Lindstedt and M. Rundgren, *J. Biol. Chem.*, 257 (1982) 11922.